ISTANBUL TECHNICAL UNIVERSITY ★ GRADUATE SCHOOL OF SCIENCE ENGINEERING AND TECHNOLOGY

MECHANICAL BEHAVIOUR OF NANOPOROUS METALS REINFORCED WITH CARBON BASED NANOMATERIALS

M.Sc. THESIS

Deniz Ezgi GÜLMEZ

Department of Mechanical Engineering

Solid Mechanics Programme

JUNE 2017

ISTANBUL TECHNICAL UNIVERSITY ★ GRADUATE SCHOOL OF SCIENCE ENGINEERING AND TECHNOLOGY

MECHANICAL BEHAVIOUR OF NANOPOROUS METALS REINFORCED WITH CARBON BASED NANOMATERIALS

M.Sc. THESIS

Deniz Ezgi GÜLMEZ
(503151507)

Department of Mechanical Engineering

Solid Mechanics Programme

Thesis Advisor: Asst. Prof. Dr. Mesut KIRCA

JUNE 2017

İSTANBUL TEKNİK ÜNİVERSİTESİ ★ FEN BİLİMLERİ ENSTİTÜSÜ

KARBON TABANLI NANOMALZEMELERLE GÜÇLENDİRİLMİŞ NANO-GÖZENEKLİ METALLERİN MEKANİK DAVRANIŞI

YÜKSEK LİSANS TEZİ

Deniz Ezgi GÜLMEZ
(503151507)

Makina Mühendisliği Anabilim Dalı

Katı Cisimlerin Mekaniği Programı

Tez Danışmanı: Asst. Prof. Dr. Mesut KIRCA

HAZİRAN 2017

Deniz Ezgi GÜLMEZ, a M.Sc. student of ITU Graduate School of Science Engineering and Technology 503151507 successfully defended the thesis entitled "MECHANICAL BEHAVIOUR OF NANOPOROUS METALS REINFORCED WITH CARBON BASED NANOMATERIALS", which he/she prepared after fulfilling the requirements specified in the associated legislations, before the jury whose signatures are below.

Thesis Advisor :	**Asst. Prof. Dr. Mesut KIRCA** Istanbul Technical University	.....
Jury Members :	**Asst. Prof. Dr. Ali GÖKŞENLİ** Istanbul Technical University	.....
	Asst. Prof. Dr. Emrecan SÖYLEMEZ Marmara University	.....
		.....

Date of Submission : **05 May 2017**
Date of Defense : **08 June 2017**

To my family,

FOREWORD

This thesis is dedicated to my family and friends. They always support me throughout all my life.

I would like to thank to my advisor Asst. Prof. Dr. Mesut Kırca for his suggestions, guidance and, support during the thesis. Also, I would like to thank to Yunus Onur Yıldız for his advise, aid and, encouragement during my master of science.

I would like to thank to Sevim Nihal Puhurcuoğlu for who has always been a precious friend for years. I would like to thank Uğur Şimşek and Ahmet Semih Ertürk for their support as well.

This thesis is financially supported by The Scientific and Technological Research Council of Turkey (TÜBİTAK) under grant number 214M638.

June 2017

Deniz Ezgi GÜLMEZ
(Mechanical Engineer)

TABLE OF CONTENTS

Page

ABBREVIATIONS

np : Nanoporous
AIREBO : Adaptive Intermolecular Reactive Empirical Bond Order
BCC : Body Centered Cubic
CBNMs : Carbon Based Nanomaterials
CNA : Common Neighbor Analysis
CNT : Carbon Nanotube
EAM : Embedded Atom Method
FCC : Face Centered Cubic
HCP : Hexagonal Close Packed
LAMMPS : Large-scale Atomic/Molecular Massively Parallel Simulator
LJ : Lennard-Jones
MC : Monte Carlo
MD : Molecular Dynamics
MWCNT : Multi-Walled Carbon Nanotube
NPGwCNTs : Nanoporous Gold with Carbon Nanotubes
NPGwFs : Nanoporous Gold with Fullerenes
NPGwNRs : Nanoporous Gold with Nanoribbons
OTHER : Undefined Crystal Structure
REBO : Reactive Empirical Bond Order
SEM : Scanning Electron Microscope
SWCNT : Single-Walled Carbon Nanotube
SLGS : Single Layer Graphene Sheet

SYMBOLS

a	: Acceleration
Al	: Aluminum
C	: Carbon
Cu	: Copper
E	: Energy
F	: Force
H	: Total Energy according to The Hamiltonian Mechanic
K	: Kinetic Energy
L	: Total Energy according to The Lagranian Mechanic
Mg	: Magnesium
m	: Mass
N	: Particle
P	: Pressure
r	: Position Vector
T	: Temperature
t	: Time
U	: Potential Energy
$\mathbf{U_1}$, $\mathbf{U_2}$, $\mathbf{U_3}$	: Body Terms
V	: Volume
ε	: Bond Energy
μ	: Chemical Energy
ρ	: Atomic Electron Density
σ	: Cutoff Distance
ϕ	: Pair Potential

LIST OF TABLES

Page

LIST OF FIGURES

Page

MECHANICAL BEHAVIOUR OF NANOPOROUS METALS REINFORCED WITH CARBON BASED NANOMATERIALS

SUMMARY

Nanomaterials have gained attention as nanoscience and nanotechnology improves. Nanoporous (np) metals have attracted considerable attention owing to their cellular morphological features at atomistic scale which yield ultra-high specific surface area awarding a great potential to be employed in diverse applications such as catalytic, electrocatalytic, sensing, mechanical and optical. As one of the carbon based nanostructures, fullerenes, nanoribbons and CNTs are also another type of outstanding nanomaterials that have been extensively investigated due to their remarkable chemical, mechanical and optical properties. In this study, the idea of improving the mechanical behavior of nanoporous metals by inclusion of the carbon based nanomaterials, which offers a new metal-carbon nanocomposite material, is examined and discussed. With this motivation, tensile and compressive mechanical behavior of nanoporous metals reinforced with carbon based nanomaterials is investigated by classical molecular dynamics (MD) simulations. Atomistic models of the nanoporous metals with ultrathin ligaments are obtained through a stochastic process simply based on the Voronoi tessellation which has been used previously in literature. According to this technique, quasi-random points are created that depends on determined distance and volume. Voronoi volumes or surfaces are obtained by using these points with Voronoi tessellation method and line segmets occur. Then, the line segments are turned into volumetric structure. Afterwards, this volumetric structure is filled with gold atoms. Therefore, np atomic skeleton are obtained. Finally, carbon based nanomaterials are added into the cellular voids to obtain final atomistic configurations for the numerical tensile and compressive tests. Several numerical specimens are prepared with different type of carbon based nanomaterials such as CNTs, nanoribbons and, fullerenes per cell. LAMMPS (Large-scale Atomic/Molecular Massively Parallel Simulator) code was used to perform classical MD simulations to conduct uniaxial tension and compression experiments on np models filled by carbon based nanomaterials. The interactions between the metal atoms are modeled by using embedded atomic method (EAM) while adaptive intermolecular reactive empirical bond order (AIREBO) potential is employed for the interaction of carbon atoms. Furthermore, atomic interactions between the metal and carbon atoms are represented by Lennard-Jones potential with appropriate parameters. In conclusion, the ultimate goal of the study is to present the effects of carbon based nanomaterials embedded into the cellular structure of np metals on the tensile and compressive response of the porous metals. The results are believed to be informative and instructive for the experimentalists to synthesize hybrid nanoporous materials with improved properties and multifunctional characteristics.

KARBON TABANLI NANOMALZEMELERLE GÜÇLENDİRİLMİŞ NANO-GÖZENEKLİ METALLERİN MEKANİK DAVRANIŞI

ÖZET

Nanoteknoloji ve nanobilim günden güne gelişen disiplinler arası bir çalışma alanıdır. Fizik, kimya, biyoloji, malzeme bilimi ve mühendislik gibi bilim dallarının birbirleriyle etkileşimi ve bu etkileşimin kendini geliştirmesiyle endüstriyel ve akademik alanda önemli bir yere sahip olmuştur ve olmaya devam etmektedir. Nanoteknolojik uygulamalar elektronik, tıp ve ileri malzeme alanlarında yaygın kullanıma sahiptir. Örneğin, elektronik uygulamalarda sensör ve bilgi depolama, tıbbi uygulamalarda ilaç tasarımı, gen ve protein analizi, ileri malzeme alanında nanokompozitler, su geçirmez ve kendi kendini temizleyebilen kumaşlar gibi uygulamalar günümüzün vazgeçilmez bir parçası olduğunun bir kanıtıdır.

Nanomalzemeler 1-100 nm ölçülerinde nano-parçacıklardan oluşur. Boyutsal özelliklerinden dolayı nanomalzemeler tıp, havacılık ve elektronik gibi bir çok alanda kullanımı yaygınlaşmıştır. Yapılan araştırmalar malzeme boyutu küçüldükçe malzemelerin yeni özelliklerinin ortaya çıktığını göstermektedir. Boyut küçüldükçe malzeme özelliklerinin iyiye gitmesinin sebebi yüzey hacim oranı artması ile daha etkili kimyasal özelliklerin ortaya çıkması ve kuantum özellikler önem kazanması ile de atom geometrisinin ve diziliminin olumlu etkilerinin belirgin hale gelmesidir. Bazı nanomalzemeler volkanik patlamalar ve orman yangınları gibi doğal yollarla oluşabilirken, çoğu nanomalzemeler özellikle mühendislikte kullanılanlar moden teknolojik yöntemlerle üretilebilmektedir. Nanomalzemelerin üretimleri alt-üst yaklaşımı ve yukarı-aşağı yaklaşımı ile iki ana yöntemle yapılır.

Son zamanlarda nano-gözenekli malzemeler de akademik ve endüstriyel alanda araştırmacıların ilgisini çekerek sensör, yakıt hücresi, aktuatör, süperkapasitör gibi çeşitli uygulamaların vazgeçilmezi olmuştur. Nano-gözenekli malzemeler kemik, biyolojik hücre doğada kendiliğinden bulunmasının yanı sıra yapay olarak da üretimi yapılabilir. Nano-gözenekli malzemelerin en önemli özellikleri düşük göreceli yoğunluğa ve yüksek yüzey hacim oranına sahip olmasıdır. Bu özellikler nano-gözenekli malzemelerin uygulama alanının artmasını sağlar. Oluşan gözenekler ağsı bir yapı meydana getirerek absorbe etme, eleme, yerleştirme ve molekül ayırma gibi çeşitli uygulamalarda önemli bir yere sahip olur. Gözeneklerin oluşturduğu çok geniş bir yüzeyin sabit hacim içinde bulunmasından dolayı nano-gözenekli malzemeler ana metalin özelliklerinden farklı özellik gösterir. Serbest yüzeyler ihmal edilemeyecek boyutlara ulaşır ve esas malzemenin özelliklerinin değişmesine neden olur. Nano-gözenekli malzemeler boşluk tipine göre açık ve kapalı hücreli olmak üzere çeşittir. Yalıtım ve depolama için daha çok kapalı hücreli nano-gözenekli malzemeler kullanılırken, sensör, katalizör ve eyleyici olarak da açık hücreli nano-gözenekli malzemeler kullanılır. Literatürde nano-gözenekli malzemeler üzerine birçok deneysel ve hesaplamalı çalışmalar bulunmaktadır. Nano-gözenekli malzemelerin biçimsel özellikleri yapılan alaşımsızlaştırma yöntemi sonucu oluşur. Bu yöntemde ikili

alaşımlardaki soy metal elektrokimyasal dağlama ile malzemeden uzaklaştırılır ve gözenekli yapı elde edilir. Deneysel olarak bu şekilde elde edilen nano-gözenekli yapı hesaplamalı inceleme için literatürde de bulunan kürelerin kesişimi ve Voronoi mozaikleme yöntemleri kullanılarak modellemesi yapılır. Bu tezde Voronoi mozaikleme yöntemi ile nano-gözenekli malzeme modeli yapılmıştır. Bu yöntemde belirlenen mesafelerle yarı rastgele noktalar belirli bir alanda oluşturulur. Bu noktalar Voronoi mozaikleme yöntemi kullanılarak Voronoi hacimler veya yüzeyler oluşturulur ve bu hacimleri veya yüzeyleri oluşturan çizgi parçaları elde edilir. Bu çizgi parçalarına hacim kazandırılarak hacimsel bir yapı elde edlilr. Elde edilen bu hacimsel yapının içi atomlarla doldurulur. Bu tezde nano-gözenekli altın geleneksel gözenekli metallere göre yüksek dayanım gösterdiği için altın atomu tercih edilmiştir.

Gelişen teknoloji ile birlikte karbon tabanlı malzemelere olan ilgi de artmaya başladı. Karbonların farklı şekilde bağ yapmasından dolayı fulleren, nanorod, nanokonik, karbon nanotüp, grafen, nanoşerit gibi çok çeşitli karbon tabanlı malzeme bulunmaktadır. Karbon nanoyapılar boyutlarına göre sınıflandırılabilir. Örneğin, nanokonik, fulleren 0 boyutlu yapılara, nanotüp, nano şerit 1 boyutlu yapılara, grafen 2 boyutlu yapılara, 3 boyutlu grafit kristali ve nanotüp ağı 3 boyutlu yapılara örnek gösterilebilir. Bu tezde, karbon nanotüpler, fullerenler ve nano şeritler kullanılmıştır. Fullerenler, 1985 yılında Kroto ve arkadaşları tarafından keşfedilmiştir. Fullerenler, içerdikleri karbon atomu sayısına göre isimlendirilirler. C_{60} ile ifade edilen fulleren 60 tane karbon atomu içerdiğini göstermektedir. Batarya, yakıt hücresi, gaz depolama, optik ve sensör uygulamalarında ve biyolojik sistemlerde kullanılan fullerenlerin en etkileyici özelliği küresel şekli ve simetrik yapısıdır. Futbol topuna benzeyen bu yapılarla yapılan çalışmalarda malzemelerin mekanik özelliklerinde olumlu etkiler oluşturulduğu tespit edilmiştir. Önemli bir karbon tabanlı malzeme olan karbon nanotüpler (KNT) ise 1991 yılında Iijima tarafından C_{60} fulleren sentezi yaparken keşfedilmiştir. Yüksek sertlik, yüksek dayanım, düşük yoğunluk, yüksek kırılma tokluğu, yüksek elektrik iletkenliği, iyi optik özellikleri ve küçük boyutu sayesinde araştırmacıların dikkatini çekerek bir çok akademik ve endüstriyel çalışma alanı olmuştur. Bir diğer karbon tabanlı malzeme ise, grafenlerden alınan kesitle elde edilen nano şeritlerdir. Bu yapılar hakkında da literatürde birçok çalışma bulunmaktadır.

Son zamanlarda araştırmacılar hesaplamalı ve deneysel olarak nanomalzemeleri karbon tabanlı malzemelerle birleştirmek ya da nano-gözenekli malzemelerde kaplama yaparak nanomalzemelerin mekanik özelliklerini arttırma çalışmaları yapmışlardır. Bu tür çalışmalar yeni nanomalzemelerin ortaya çıkmasını sağlayarak daha iyi mekanik ve elektriksel özelliklere sahip nanokompozitler elde edilmiştir. Bu tezde, nanogözenekli malzemelerin gözeneklerine karbon tabanlı nanomalzemler eklenerek moleküler dinamik simülasyonlarının yardımıyla mekanik özelliklerinde oluşan değişimler incelenmiştir. Moleküler dinamik yöntemi istatistiksel mekaniğe bağlı olan deterministik bir yöntemdir. Bu yöntemde, atomların denge ve yörüngeleri Newton'un ikinci yasası uygulanarak etkileşen atomların zamana göre davranışı dikkate alınarak hesaplanır. Atomik simülasyon yöntemi işlem öncesi, analiz ve işlem sonrası olmak üzere üç aşamadan oluşur. İşlem öncesi aşamada, basınç ve sıcaklık gibi başlangıç koşulları belirlenir. Sayısal integrasyonda Newton'un ikinci yasası uygulanarak her bir atomun hızı ve anlık konumları belirlenen sisteme tanıtılır. Analiz aşamasında, farklı termodinamik koşullar altında uygun atomlar arası potansiyellere göre kuvvet ve enerji hesaplamalarına devam edilir. İşlem sonrası aşamasında ise, sayısal ölçüm sonuçları görüntülenir ve yazdırılır.

Bu tezde, modeller iki ana yapının birleşimi ile elde edilir. İlk yapı karbon tabanlı nanomalzemelerin oluşturduğu ağ yapısıdır. Bu ağ yapısında öncelikle belirli bir hacime belli mesafelerde olacak şekilde rastgele noktalar atanır ve bir nokta bulutu elde edilir. Bu nokta bulutlarına karbon tabanlı nanomalzemeler yerleştirilir ve karbon tabanlı malzemelerin bulunduğu bir hacim elde edilir. Elde edilen bu hacimden Voronoi mozaikleme yöntemi ile elde ettiğimiz nano-gözenekli yapının kesiştiği hacimler silinir ve ortaya istediğimiz ağ yapısı ortaya çıkar. Nano-gözenekli yapı ile bu ağ yapısını birleştirerek yeni nanokompozit malzememizi oluşturmuş oluruz. Fulleren, KNT ve nano şeritler kullanarak üç farklı modellin çeki ve bası yükleri altındaki mekanik davranışlarının hem birbirleriyle hem de nano-gözenekli yapıyla karşılaştırılması yapıldı. Çekme testi sonucu elde edilen çekme-birim şekil değiştirme eğrisi üzerinden yapılan karşılaştırmalar yardımıyla karbon tabanlı nanomalzemelerin np altın üzerindeki etkisi incelendi. Aynı karşılaştırma tek eksenli basma gerilmesi üzerinde de yapıldı. Ayrıca, yapıların tek ekesenli çeki ve bası yükleri altında komşu atom analizi yapılarak karbon tabanlı malzemelerin np altının atomik yapısında herhangi bir değişim olup olmadığı da incelenmiştir. Aynı zamanda farklı gerinim oranları uygulanarak çeki ve bası gerilmeleri altındaki mekanik özellikleri de incelendi.

Tez beş ana bölümden oluşmaktadır.İlk bölümünde nanomalzemeler, nano-gözenekli malzemeler, karbon tabanlı nanomalzemeler hakkında bilgi verilerek konuya giriş yapılmıştır. İkinci bölümde, moleküler dinamik simülasyonları üzerinde durularak nanogözenekli yapıların incelenmesinde kullanılan çözüm yöntemlerine değinilmiştir. Üçüncü bölümde, modellerin nasıl oluşturulduğu ve oluşturulan modellerin simülasyon şartlarının nasıl uygulandığı üzerinde durulmuştur. Dördüncü bölümde, elde edilen sonuçlar incelenerek yorumlanmıştır. Son bölümde ise, yapılan çalışma değerlendirilmiştir ve gelecek çalışmalar için önerilerde bulunulmuştur.

1. INTRODUCTION

Nano means "dwarf" in Greek [18]. 1 nanometer is one bilionth of a meter in units of measure.Nanotechnology and nanoscience are interdisciplinary branch of science such as physics, chemistry, material science, biology, engineering that improve day by day itself and have important place in all fields from fundamental sciences to engineering for the nanoscale [19]. Besides, Miyazaki and Islam [20] investigated statictically improvement of nanotechnology both academia and industry according to continents and countries. The dimension comparison of the nanoscale from water molecule to tennis ball is as shown in Figure 1.1.

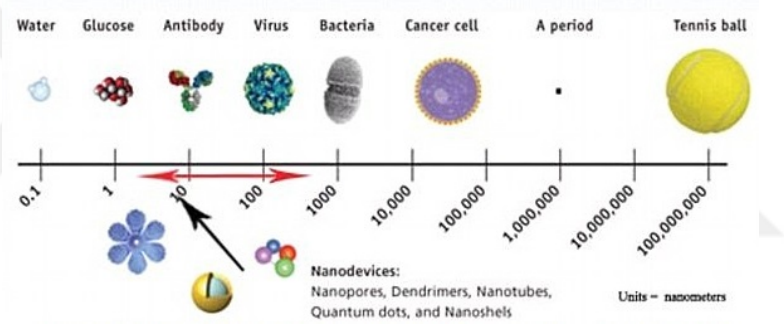

Figure 1.1 : Nanometer-Sized Comparison [3].

In recent years, interest in nanomaterials and nanostructures have also increased and the studies in this regard have begun to gain importance [21]. Nanotechnology applications exist in many technological areas such as electronics, biotechnology and advanced materials. For instance, sensors and information storage for electrical applications, drug design, gene and protein analysis for medical applications, nanocomposites, waterproof fabrics and environmental clean-up for material development applications [20].

1.1 Nanomaterials

Nanomaterials or nanostructured materials compose of nano-scale particles that are in the range of 1 to 100 nm. Nanomaterials have attracted attention a lot of field such as medicine, aerospace and electronics because of their interesting properties on the

size.Reserch shows that when size of a material is smaller, new features of material are revealed. The differences in the structures of the nano-scale are not only related to the small size, but also to the apperance of different physical properties in small sizes [22]. This difference is based on two main reasons. The first reason is that the surface area increases significantly,namely high surface to volume ratio and, consequently, the nano-scaled structures is exposed to greater chemical reactions. Thus, mechanical, electrical and thermal behavior of the material are affected and changed. For instance, cadmiyum seleride (CdSe) quantum dots have different colour according to their sizes and shapes under the light [23]. The other reason is that quantum properties are more prominent in atomic scale. This affects the geometry and arrangement of atoms. For example, it has been observed that as the scale of gold metal decreases, the Yield Strength of gold increases [24]. While some nanomaterials take place naturally such as volcano eruptions and forest fires, most of nanomaterials especially engineering nanomaterials are manufactured by modern technological methods.

Table 1.1 : Typical nanomaterials [1]

	Size (approx.)	Materials
(a) Nanocrystals and clusters (quantum dots)	diameter 1-10 nm	Metals, semiconductors, magnetic materials
Other nanoparticles	diameter 1-100 nm	Ceramic oxides
(b) Nanowires	diameter 1-100 nm	Metals, semiconductors, oxides, sulfides, nitrides
Nanotubes	diameter 1-100 nm	Carbon, layered metal chalcogenides
(c) 2-Dimensional array (of nano particles)	several $nm^2 - \mu m^2$	Metals, semiconductors, magnetic materials
Surfaces and thin films	thickness 1-1000 nm	Various materials
(d) 3-Dimensional structures (superlattices)	Several nm in all three dimensions	Metals, semiconductors, magnetic materials

Nanomaterials have begun becoming a part of life with developing technology day by day, such as cosmetics, tires, electronics, sporting goods [25]. For instance, new materials are obtained that have better properties by combining different nanomaterials for application of materials science. Treatment of various hereditary diseases are developed with gene and protein analysis that use DNA chip [20]. Thanks to the nanomaterials, the devices used for data storage are smaller. Thus, more imformation can be stored in a smaller space which is a proof that nanomaterials are also actively involved in the computer science. The use of nanocrystalline

materials can better monitor the quaility of drinking water, properties of products and materials by increasing the selectivity of sensors [20]. Nanostructured materials can be categorised according to nıumber of nanomaterials dimension. In this respect, nanomaterials such as quantum dots, onions, core-shell nanoparticles, are classified 0-dimensional nanomaterials [4]. Nanowires, nanotubes, nanoribbons, and nanorods are examples of 1-dimensional nanomaterials [4]. In the same way, nanoplates, nanosheets and nanodisks are nanomaterials in 2-dimensions [4]. Finally, nanocoils, nanoflowers, nanocones, and nanopillers are regarded 3-dimensinal nanomaterials [4]. According to some sources the 3-dimensional nanomaterial classification is included in the 0-dimensional nanomaterials [23]. There are some examples of nanomaterials according to dimension in Fig.1.2-5.

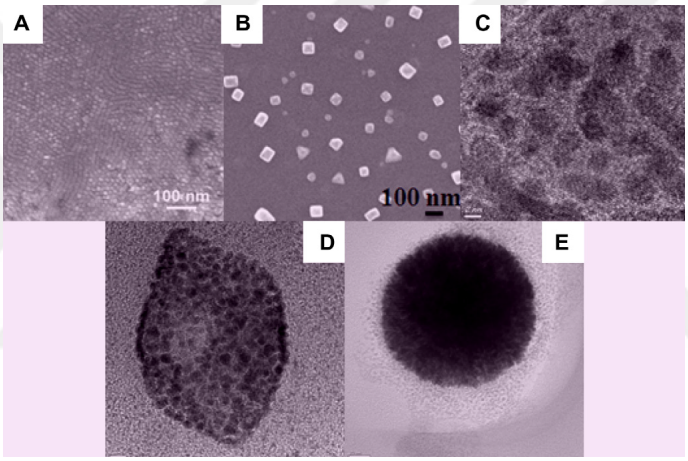

Figure 1.2 : Examples of 0D nanomaterials. (A) Quantum dots, (B) nanoparticles arrays, (C) core–shell nanoparticles, (D) hollow cubes, and (E) nanospheres [4].

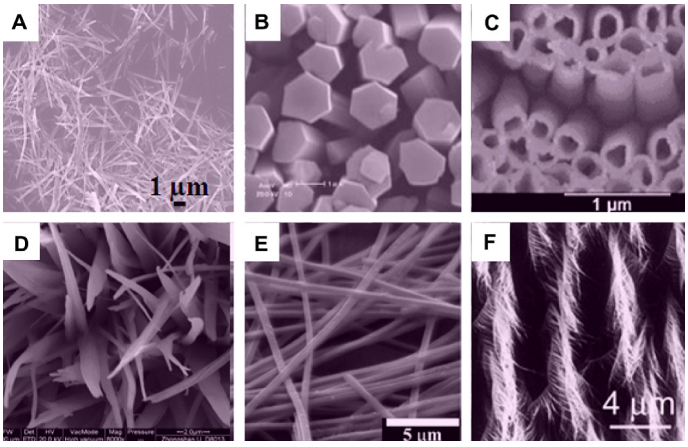

Figure 1.3 : Examples of 1D nanomaterials. (A) Nanowires, (B) nanorods, (C) nanotubes, (D) nanobelts, (E) nanoribbons, and (F) hierarchical nanostructures [4].

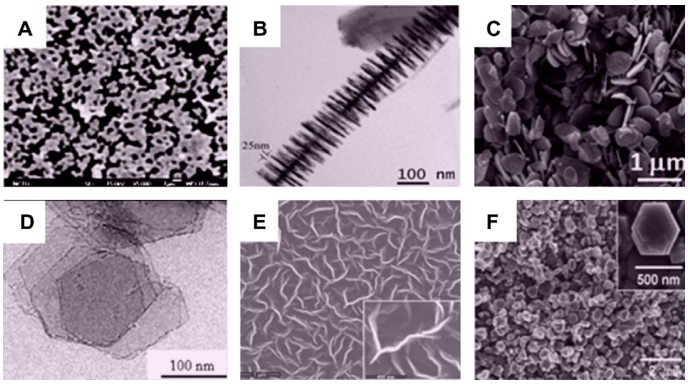

Figure 1.4 : Examples of 2D nanomaterials.(A) Junctions (continuous islands), (B) branched structures,(C) nanoplates, (D) nanosheets, (E) nanowalls,and (F) nanodisks [4].

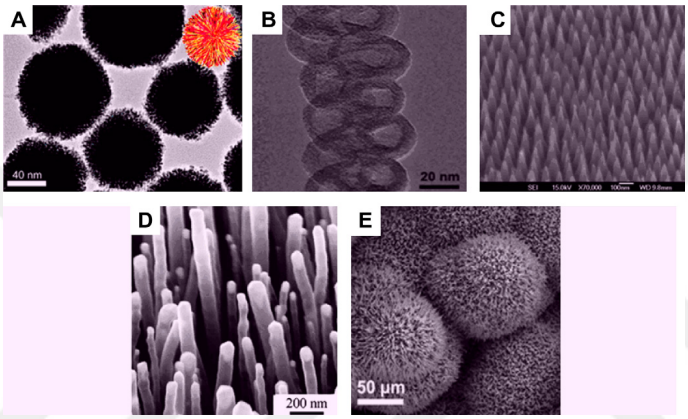

Figure 1.5 : Examples of 3D nanomaterials.(A) Nanoballs (dendritic structures),(B) nanocoils, (C) nanocones, (D) nanopillers, and (E) nanoflowers [4].

As it shown in Fig.1.6, manufacturing and synthesis of nanomaterials are used two main approaches which are bottom-up and top-down methods. Nanostructured materials are fabricated from the molecular level manupulations in the bottom-up approach that has konwn by chemists. Structural units of atomic scale such as atoms, molecules and clusters, are arranged similarly more complicated structural units to the growth of a crystal. When it comes to top-down approach, nanostructures are constructed from macro-level materials rather than molecular level. Fabrication examples of top-down approach are laser ablation, nano-lithography, physical vapor deposition, miling and hydrothermal technique [26].

Bottom-up approaches search to have smaller parts regulate themselves more complicated combination, whereas top-down approaches search to build nanostructuralcomponents by using larger parts. An disadvantage of top-down methods cannot supply uniform structures at very small sizes. However, bottom-up methods can

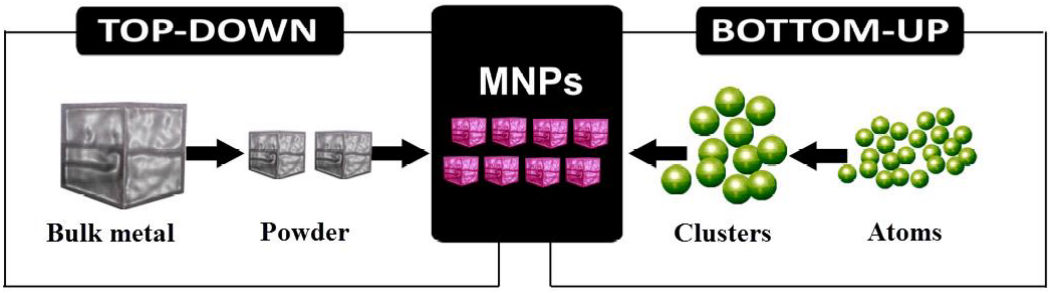

Figure 1.6 : Scheme of Top-Down and Bottom-up approaches to the synthesis of metal nanoparticles [5]

produce uniform structures. In spite of this drawback, top-down approaches have importance for development of nanotechnology and nanoscience.

1.2 Introduction to Nanoporous Materials

Recently, nanoporous (np) materials have attracted high interest in academical and industrial research area, due to their substantial properties to be employed within a wide range of various applications such as sensors, actuators, fuel cells, catalysis, and supercapacitors. Np materials can be artifically manufactured as well as they exist in nature such as structure of bones and biological cells. Artifical np materials are studiously fabricated with taking into account of morphological parameters such as size and distribution of pore, porosity and chemical properties [8]. The most significant properties of np materials are having low relative density and high surface to volume ratio. For this reasons, np materials allow being a significant candidates in wide range applications such as sensors, separators, actuators, photonic crystals and bio-implants.

Morphological properties of np metals are basically stem from the mostly-used manufacturing method, namely dealloying, which is electrochemically driven etching process to removeless noble elements within the dual alloys. The reorganization of the more noble elements by the surface diffusion accompanied with phase transformation yields the unique porous microstructure presenting the combined properties of both metals and nanostructured metals. Among these nanostructures, np gold that is also termed as the prototype of np metals is the most popular np metal on which many experimental and theoretical studies are performed owing to its significant structural stability and biocompatibility as well as its excellent electrical conductivity, good permeability for gas or liquid molecules. Figure 1.7 presents several examples of

complex np structures. Their structures are similar to a network of ligaments with diversifying cross sections intersected with each other forming joints throughout the network. The most significant useful properties of np materials take place their structural network of pores, which permit them important candidates in various applications such as adsorbing, sieving, accommodating and separating molecules. Therefore, np materials are diversified than other nanomaterials owing to that serviceable features of np materials are considerably influenced by characteristics of nanopores or nanocells such as pore shape, intensity and size besides the surface and bulk properties of primary materials.

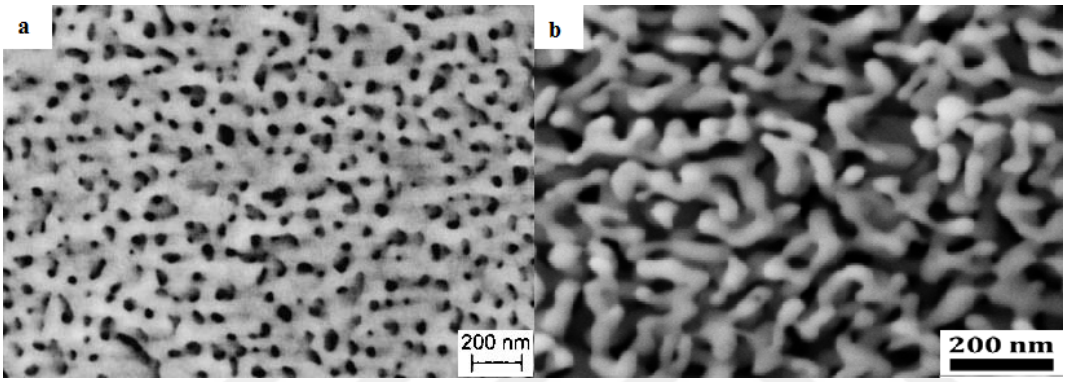

Figure 1.7 : Morphologies of nanoporous materials: (a) Nanoporous Platin [6] (b) Nanoporous Gold [7].

Due to this important properties of their, various academic studies have been carried out by attracting the attention of many researchers and they are being continued. Researchers have interested np materials in working on sensors, actuators, catalysis and supercapacitors [27–30], but recently they have studied on mechanical properties of their. For instance, Biener et al. explored the Young's modulus and hardness of nanoporous gold experimentally by conducting nanoindentation tests and examining the microstructure thorough scanning electron microscope (SEM) [31]. Furthermore, tension and compression tests were performed on sub-millimeter gage thicknesses of nanoporous gold by Balk et al. [32]. They showed that the compressive strength was higher than the tensile strength, while all strength values were found to be significantly lower than the values obtained from the nanoindentation tests presented in literature. In a different study, Briot et al. [33] investigated the mechanical behavior of single crystalline nanoporous gold on millimeter-scale and demonstrated that the Young's modulus values measured from the tension and compression tests are lower than the

values of nanoindentation test. Another experimental study carried out by Lee et al. [34] focused on the Young's modulus, residual stress and yield stresses which were measured with the help of both tensile and nanoindentation tests. In addition to the experimental studies, numerical studies on the mechanical behavior of nanoporous gold can also be found in literature. One of them presented by Sun et al. [35] investigated deformation mechanisms of nanoporous gold subjected to uniaxial tensile loading by modeling the nanoporous structure using the atomistic modeling technique developed by Crowson [36]. Moreover, they also suggested scaling laws based on the relative density for the effective Young's modulus, yield stress, and ultimate strength of nanoporous gold. Similarly, Rodriguez-Nieva et al. [37] studied the compressive behavior of nanoporous gold by using molecular dynamics simulations and investigated the stress distribution, dislocation and stacking fault network of nanoporous gold. Recently, Yildiz and Kirca [38] examined the mechanical behavior of coated and uncoated nanoporous gold subjected to uniaxial tension by using a novel atomistic modeling technique based on Voronoi tessellation [39]. The effect of coating thickness and material types on the deformation mechanisms were investigated by examining the microstructural evolution of the structures.

1.2.1 Mechanics of Macroporous Foams

Foams or cellular solids can be described as combination which includes three dimensional randomly distributed cells that are interconnected struts and/or plates. Cellular solids are categorized as open cell and closed cell foams according to material distribution, as shown in Figure 1.8. If the cells are interconnected with each other and plate-like surfaces closing the surfaces of the cell do not exist, the foam are called an open cell foam. In closed cell foams, the cells are not interconnected with each other owing to plate/shell like walls between the cells. Due to the fact that most of np materials consist of open cell structures, open cell foams are investigated in this dissertation.

Main propose of these micromechanical models for examining mechanical properties is to obtain initial elastic constant such as the Young's modulus E^*, shear modulus G^*, Poisson's ratio ν^*, by the unit cell models considering the ligaments of the cells as structural beams and using definition of elastic constants in the classical strength of

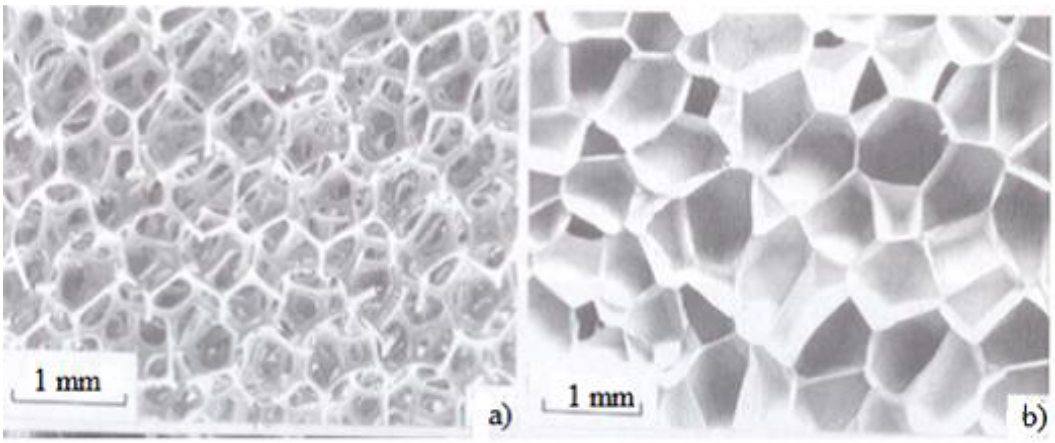

Figure 1.8 : (a) Cellular structure of open cell polyurethane , (b) Close cell polyethylene [8]

materials. Gibson and Ashby [8] have studies as to investigate mechanical properties of cubic unit cell structure (in Figure 1.9).

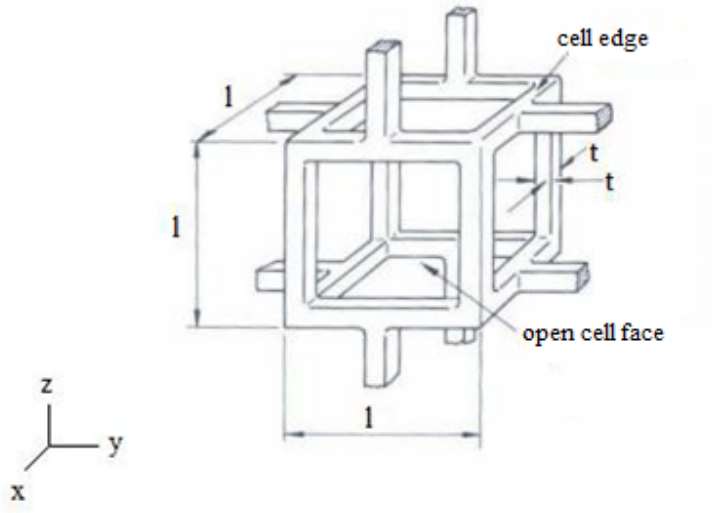

Figure 1.9 : A cubic structure for an open cell foam [8]

The equation of this cubic unit cell model with relationship between the Young's modulus, yield strength and relative density of open cell foam can be construct as follows:

$$\frac{E^*}{E_s} = C_1 \left(\frac{\rho^*}{\rho_s} \right)^2 \tag{1.1}$$

$$\frac{\sigma^*_{pl}}{\sigma_{ys}} = C_2 \left(\frac{\rho^*}{\rho_s} \right)^{\frac{3}{2}} \tag{1.2}$$

where are ρ^* and ρ_s the density of foam and desity of the bulk solid material, respectively. Likewise, E^* and σ^*_{pl} are the Young's modulus and plastic yield strength (the plastic-collapse strength) of the foam respectively, while E_s and σ_{ys} are the Young's modulus and yield strength of the bulk solid material.(ρ^*/ρ_s) represents the relative density of foam.C_1 and C_2 are coefficient that approximately equal to 1 and 3/8 according to obtained data experimentally [8].

The mechanical behaviour of foams under the uniaxial compressive stress shows in Figure 1.10. The stress-strain curve consists of three region. The first part of the graph refers to the linear elastic region, the second region refers to plastic yielding (namely the work hardening region) region and the last region refers to the densification region.

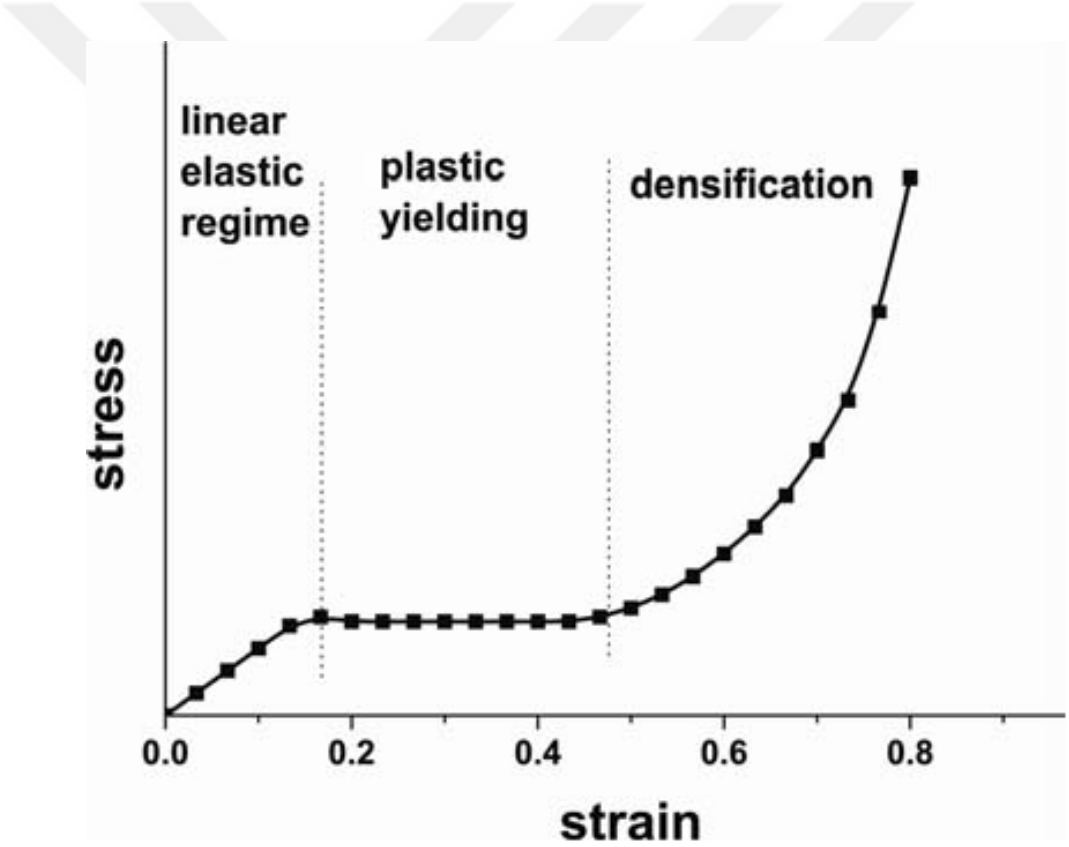

Figure 1.10 : Compressive stress-strain behaviour of a metal foam [28].

Technique of indentation is most common experimental method to examine yield strength and hardness of cellular solids. The yield stress is approximately equal to one third of the hardness $(H \sim 3\sigma_y)$ for bulk materials, whereas the yield stress is almost equal to the hardness $(H \sim \sigma_y)$ for low density foams $(\rho^*/\rho_s \leq 0.3))$ [8].

1.2.2 Mechanics of Nanoporous Foams

Nanoindentation is a measure method that investigates mechanical properties of nanporous materials. The advantage of nanoindentation technique is to be simple and to have low requirement such as sample size, defect concentration (in Figure 1.11. The yield stress is assumed to be approximately equal to the hardness of nanoporous materials ($H \sim \sigma_y$) [8].

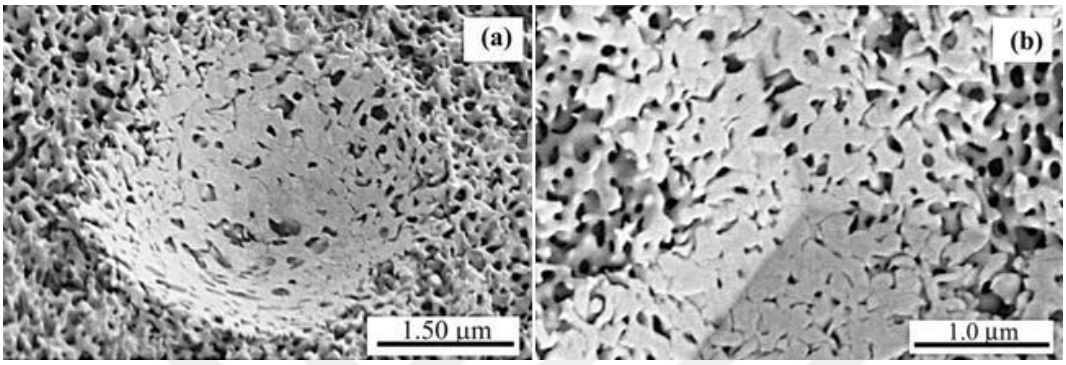

Figure 1.11 : SEM micrographs of 8000-mN indentations on a fractured surface of np gold: (a) conospherical tip with a tip radius of 0.1 mm, and (b) Berkovich tip with a curvature of 200 nm. Ductile densification is observed for both probes. Note that the plastic deformation is confined to the area under the indenter, and adjacent areas are virtually undisturbed [9].

There are both computational and experimental studies about size effects on the mechanical properties of nanoporous materials. For example, Biener et. al. [10] made comparison gold foam between nano and macro scale. And, they obtained thatin contrast to macroporous foams, the yield strength of np Au increases significantly as size of ligaments decreases. Figure 1.12 shows size effect of np Au with relative density values ranging from 0.2 to 0.42 on the yield stress. As a result, np Au foam can be imagine as a three-dimensional network of ultrahigh strength nanowires. In this manner, structure that have high strength and high porosity is obtained [10].

Hakamada and Mabuchi [40] developed a relationship between the yield stress of Au ligament and size of ligament by using the Eq 1.3 where d_1 is ligament size, K is a constant and m is ligament size.

$$\sigma_{ys} = K d_1^m \tag{1.3}$$

The value of m is approximately -0.20 in np Au [40]. And also, Hakamada and Mabuchi [40] thougth that grain refinement strengthening and dimensional restraint

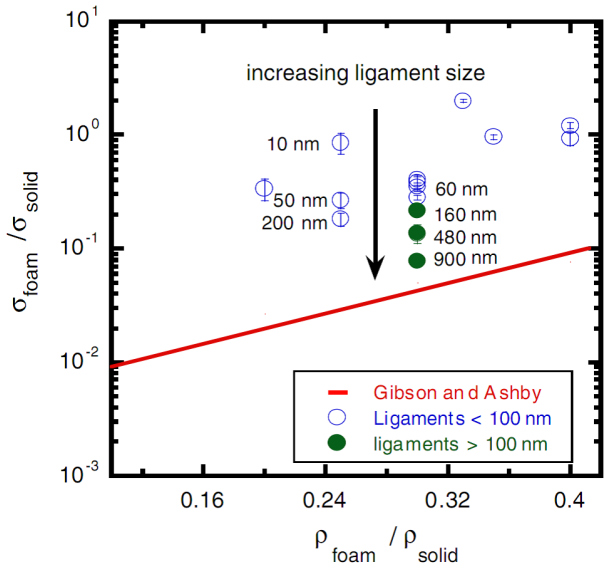

Figure 1.12 : Effect of ligament sizes and relative desity on the yield stress for np Au. The solid line presents calculated results for metal foam, while the symbols are represent experimantal results np Au [10].

theory for metals at micro scale were improper for explaining the high strength of np Au and the yield stress of np Au according to the ligament size can be compare with FCC (Face Centered Cubic) nanowires.

1.3 Carbon Based Nanomaterials

In recent years, interest in carbon-based nanomaterials has increased with advancing technology. There are lots of type carbon based materials, as shown in Figure 1.13. A wide variety of carbon based materials such as fullerenes, carbon nanotubes (CNT), graphenes are formed by the bonding of the carbons to each other in different combinations. Carbon nanostructures can be categorized according to their dimensions which are 0-dimensional structures such as fullerenes, nanocones, 1-dimensional structures such as nanotubes, nanoribbons, 2-dimensional structures such as graphenes and 3-dimensional structures such as 3D graphite cyristal and 3D nanotube networks [11].This thesis focuses on three types of carbon based materials: Fullerenes, carbon nanotubes,graphenes and nanoribbons.

1.3.1 Fullerenes

Buckminsterfullerene or C_{60} was discovered in 1985 by Kroto and colleagues [41]. Fullerenes are used many applications such as battery and fuel cells [42], gas storage

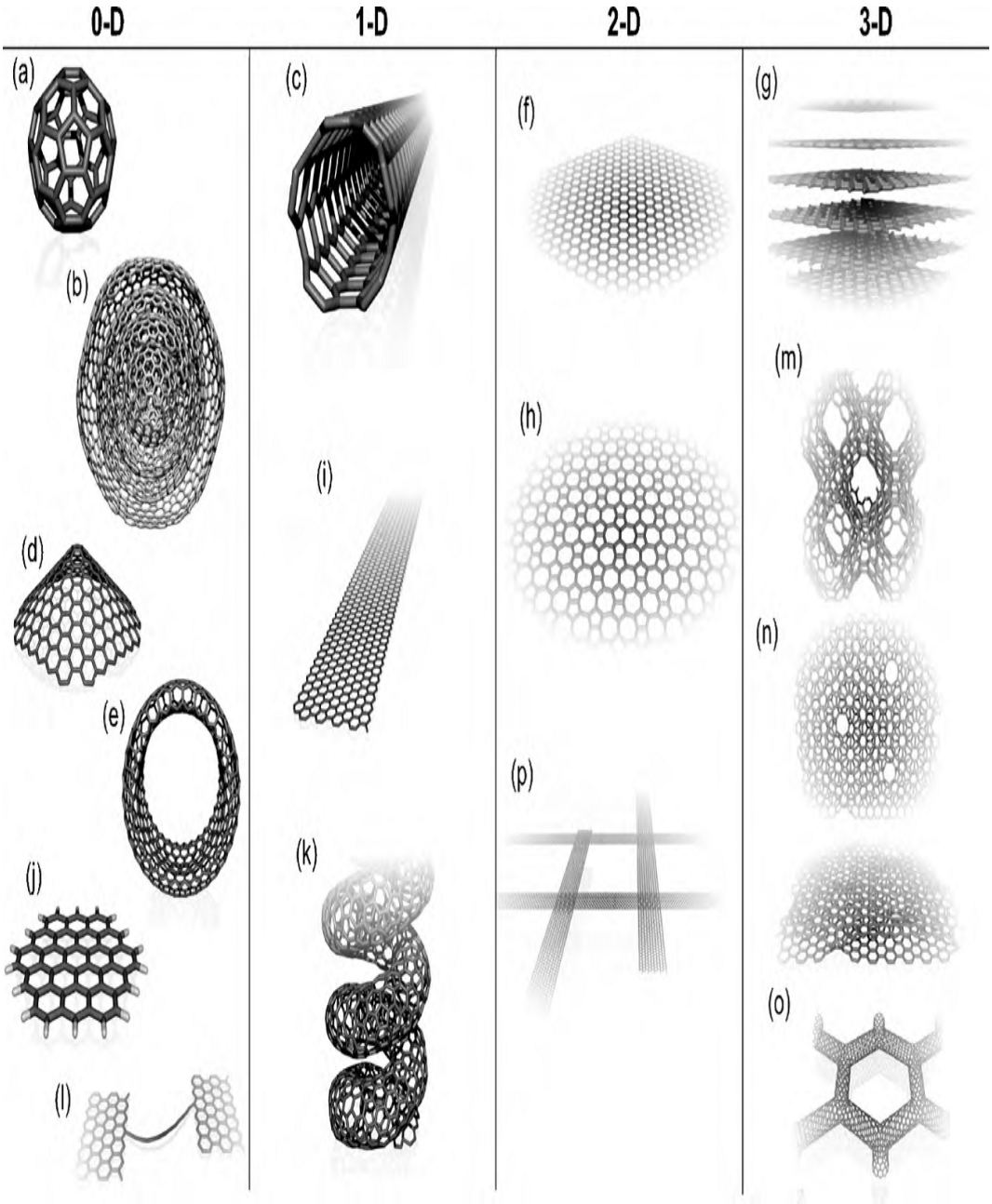

Figure 1.13 : Carbon based nanomaterials: (a) C_{60}: Buckminsterfullerene; (b) nested giant fullerenes or graphitic onions; (c) carbon nanotube; (d) nanocones or nanohorns; (e) nanotoroids; (f) graphene surface; (g) 3D graphite crystal; (h) Haeckelite surface; (i) graphene nanoribbons; (j) graphene clusters; (k) helicoidal carbon nanotube; (l) short carbon chains; (m) 3D Schwarzite crystals; (n) carbon nanofoams (interconnected graphene surfaces with channels); (o) 3D nanotube networks, and (p) nanoribbons 2D networks [11].

[43, 44], optical and sensor applications [45, 46] and biological systems [47]. The most attractive properties of C_{60} are spherical shape and high symmetry. Thanks to sp^2 nanostructures of carbon, the versatility of carbon are enabled to generate different shapes of fullerenes and other carbon based nanomaterials as seen in Figure 1.14. Buckminsterfullerene has a shape resembling a soccer ball and consists of 12 pentagonal and 20 hexagonal faces symmetrically [48].

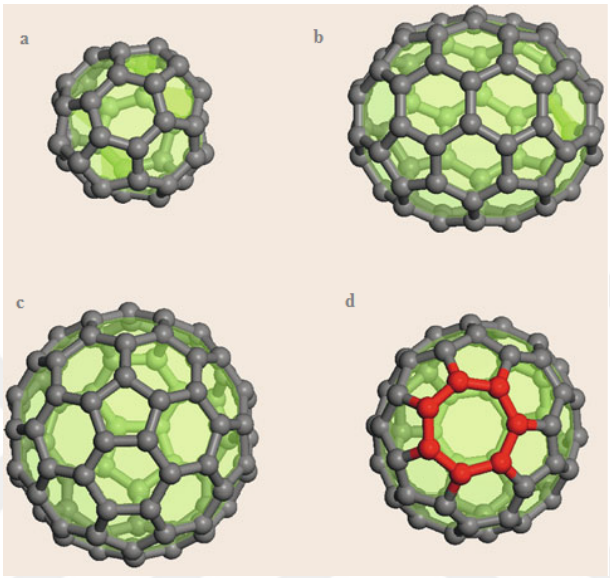

Figure 1.14 : (a) C_{40} (b) C_{70} (c) C_{80} (d) C_{62} [12].

Fullerenes are used increasing strength of nanomaterials as well. For instance, Wang [49] examines torsional instability by filling CNT with fullerenes and obtains that the critical torsion angle increases with van der Waals effect between fullerene and CNTs and the stability enhances. Zuevet. al. [50] investigate effect of fullerenes and carbon based nanomaterials on thermoreactive and thermoplastic matrices. It is observed that while there is no effect on thermoreactive matrices, the Young Modulus of thermoplastic matrices increases, especially for mixture of C_{60}/C_{70}. Barrera et. al. [51] obtained that the hardness of Al/C_{60} increases compared to pure aluminum but is below the hardness of the aluminum alloys. Shin et. al. [52] achieve that Al/C_{60} has better mechanical and damping properties than pure aluminum. Brenner et. al. [53] studiedthe resistance of C_{60} against pressure by using Molecular Dynamic Simulations.

1.3.2 Carbon Nanotubes (CNTs)

CNTs were discovered by Iijima while synthesis of fullerene C_{60} [54].Shape of CNTs resembles a rolled graphene sheet and consists of benzene-type hexagonal carbon atom

circle. Three neighbour carbon atoms are connected with covelent bonds in periodic hexagonal pattern. Therefore, CNTs have very good properties such as high stiffness, high strength, low density, high fracture toughness, high electrical conductivity, small size and good optical featues.

As shown in Figure 1.15, C_h represents roll-up vector or chiral vector that is defined as a linear combination of the unit translational vectors in the hexagonal lattice [2].

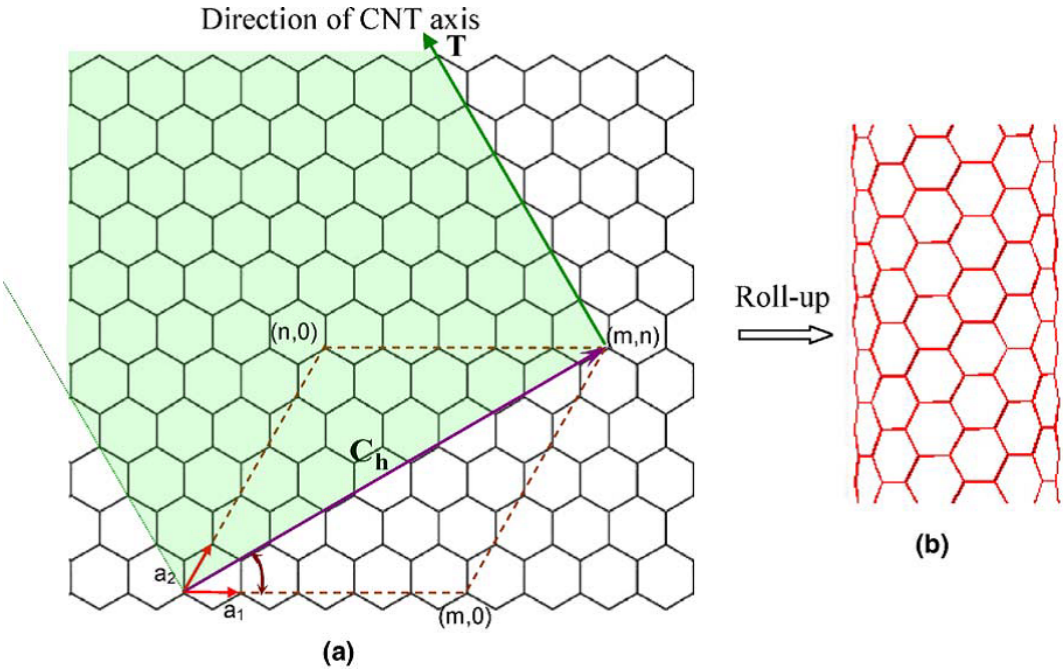

Figure 1.15 : a) Graphene Sheet with roll-up vector, b) CNT [2].

m and n are integers to describe size of CNT, a_1 and a_2 are vectors to define chiral directions. Calculation of the angle between C_h and a_1 that is called chiral angle is shown Eq 1.4 [55].

$$C_h = ma_1 + na_2 \tag{1.4}$$

$$\theta = \arcsin\left(\frac{\sqrt{3}m}{2(\sqrt{m^2+mn+n^2})}\right) \tag{1.5}$$

There are three types of single walled carbon nanotube (SWCNT) according to the chirial angle as seen in Figure 1.16.

If the CNT is called as zig-zag, it means that chiral angle is equal 0° and n value is equal zero; if the CNT is named as Armchair , the chiral angle is equal 30°; and lastly if the angle is a value that is between 0° and 30° and m is not equal but n and zero, the nanotube is called chiral, as seen in Table 1.2. They may also exist as single or multi layered structures.

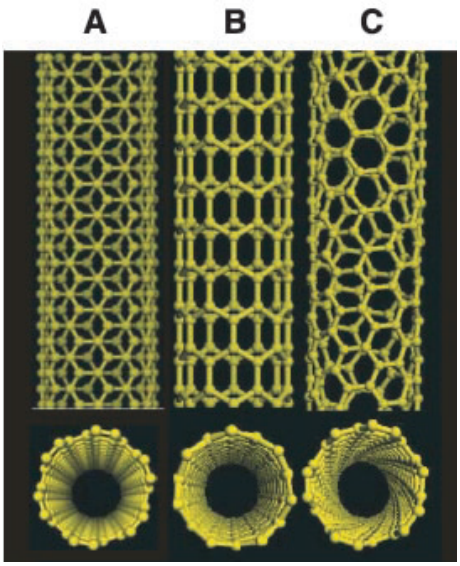

Figure 1.16 : Schematic illustrations of the structures of (A) armchair, (B) zigzag, and(C) chiral SWNTs [13].

Table 1.2 : Types of CNTs according to chiral indices [2].

Type of nanotube	Chiral indices: (m,n)	Chiral angle, θ	Tube diameter, D_{NT}
Zig-zag	(m,0)	0	$\frac{a_0 m}{\pi}$
Armchair	(m,m)	30°	$\frac{\sqrt{3}a_0 m}{\pi}$
Chiral	(m,m); m $\neq$ n $\neq$ 0	$0 < \theta < 30°$	$\frac{a_0\sqrt{m^2+mn+n^2}}{\pi}$

There are many studies on investigation of mechanical properties of CNTs. For instance, Treacy et. al. [56] examined Young's Modulus of multi-walled CNTs (MWCNT) according to length and diamater of nanotubes and they obtained that average value of Young's modulus is 1.8 TPa. Yu et. al. [57] investigated mechanical properties of SWCNTs and they attained value of Young's Modulus is range from 0.32-1.47 TPa, finally, on average 1 TPa.

1.3.3 Graphenes and Nanoribbons

Graphene is considered as a fundamental construction for carbon-based materials of all dimensions. Graphene is an atomic sheet that include a hexagonal network of sp^2 covalently bonded carbon atoms and has strong and high weight to surface ratio. Young's modulus and thermal conductivity of Graphene sheets is 1.06 TPa and 3000 $Wm^{-1}K^{-1}$ respectively [58].The Young's modulus of graphene is smaller than CNT(5,5) [59]. Nanoribbons are cut from graphene sheets. There are a lot of study about examining mechanical properties of nanoribbons. For instance, Faccio et. al. [60] investigated mechanical, electronic and structural properties of zigzag

graphene according to widths and they obtained that the Young's modulus increases as the width increases. Tabarraei et. al. [61] examined mechanical behaviour of nanoribbons according to zigzag and armchair structures.

1.4 Composite Materials Reinforced with Carbon Based Materials

In recent years, the idea of enhancing the properties of metals with carbon based nanomaterialsis in favor of researchers. Many of those studies are focused on the reinforcement of metal matrices employed within the nanocomposites. For instance, Tjong [62] presents a review study concentrating on the manufacturing, characterization and applications of metal-matrix (i.e. aluminum, magnesium, and transition metals) composites reinforced with carbon nanotubes and graphene nanosheets. There are several computational and experimental investigations for the mechanical properties of reinforced metals with carbon based nanomaterials.For instance, Silvestre et al. [63] studied the compressive mechanical behavior of single-crystal Al through MD simulationsand showed that the Young's modulus of the CNT-Al composite increased while yield stress and strain were not enhanced. Specifically, it was noted that as a result of CNT reinforcement, stiffness of single crystal Al could be improved by approximately 50% or100% depending on the loading conditions. Furthermore, Song and Zhaet al. [64] examined the tensile characteristics of gold matrix reinforced with nickel-coated and uncoated armchair SWCNTs (i.e. single walled carbon nanotubes)which are positioned in two different arrangements (i.e. parallel and vertical). As a result of MD simulations, they reported that the elastic modulus and pullout stress of embedded nickel-coated SWCNT-goldcomposite were higher than uncoated SWCNT-gold composite and single crystal gold. Along the same line, Song and Zha [65] presented the similar results in a different study for the single crystal aluminum instead of gold. Besides, the effects of the reinforcement provided by the single layer graphene sheets (SLGSs) and CNTs within the copper based nanocomposites under uniaxial tensile loadings were investigated by Bashirvand and Montazeri [66]. They indicated that SLGSs were more effective than CNTs in terms of enhancing Young's modulus and yield strength owing to their higher load transfer capability. While the majority of the studies are concentrated on the embedding of carbon based nanofillers within the metal matrix material, there are some other studies

working on the carbon based nanostructures filled by metals. For instance, Guo et al. [67] performed MD simulations to study on the deformation behavior of Au-filled SWCNTs subjected to uniaxial compressive loading. Based on their simulation results, it was demonstrated that the buckling strength of Au-filled CNTswas superior to the hollow CNTs. Apart from those numerical investigations, there are also experimental studies focusing on the strengthening effect of carbon based nanofillers. For example, Tsai and Jeng [68] examined the mechanical properties of CNT/Cu(copper) composites not only numerically but also experimentally by revealing the significance of the slenderness ratio of the CNTs within Cu matrix for the buckling performance. CNT-Cu composites were also investigated by Yoo et al. [69] presenting that the mechanical properties of CNT/Cu composites were dependent on the manufacturing technique as well as process parameters. In this regard, Munir et al. [70] reviewed the effects of several manufacturing techniques including mechanical alloying and powder metallurgy on the mechanical properties of CNT reinforced titanium-based metal composites. Furthermore, by utilizing a novel manufacturing process Deng et al. [71] fabricated CNT-Al composites with different CNT weight ratios and established the strengthening effect of CNTs by analyzing the microstructural changes and discussing the failure mechanisms of composites.Likewise, in literature there are also several experimental investigations on the mechanical behavior of different nanocomposites including Al/graphenes [72–74] and Mg/CNTs [75]. In addition to the metal matrix materials, polymers were also preferred as matrix material to be reinforced by carbon based nano fillers such as graphene and CNTs [76–78].

1.5 Purpose of Thesis

The main purpose of this thesis is to enhance mechanical properties of nanoporous metals to use carbon based nanomaterials. It is intented to generate a novel materials by taking advantage of both nanoporous materials and carbon based nanomaterials. The effects of using different carbon based nanomaterials were investigated on mechanical behaviour. The mechanical features are improved by using defected carbon based materials to establish bond between carbon atoms.

2. MOLECULAR DYNAMICS SIMULATIONS

Computational studies have begun to gain importance with the development of computer science. Computational methods are more advantageous than experimental methods in terms of time and cost. Computer simulations acts as a bridge between experiments and theories in especially multi-particle systems [79]. Monte Carlo (MC) method and molecular dynamics (MD) method are most popular computer simulation techniques. If the model is complicated and, nonlinear and parameters are uncertain, MC methods is suitable to use in solution of this type problems with random numbers and possibilities independently from time. Namely, MC method is an indeterministic simulation method [14]. Although MC method is indeterministic, MD method is deterministic which depend on statistical mechanics. The equilibration and trajectory are calculated according to set of interacting atoms with time step by applying Newton's second law [80]. Atomistic simulation processesconsists of three steps in MD simulations: pre-processing, analysis and post-processing. Firstly, initial conditions such as pressure, temperature etc. are decided. Velocity and instant location of each atom in a definite system is determined implementing Newton's law in numerical integrations. Then, calculation of force and energy are carried on according to suitable interatomic potentials under different thermodynamic conditions. Finally, results of measured quantities are visualized and printed. MD is based on clasical mechanic law such as Euler, Hamilton, Lagrange and especially Newton's second law [80]. V is the atomic potential, F_i is the forve owing to interaction of atoms which express as the gradients of potential, mi and ai are mass and acceleration of atoms, respectively.

$$F_i = m_i a_i \tag{2.1}$$

$$a_i = \frac{d^2 r_i}{dt^2} \tag{2.2}$$

$$F_i = \Delta_i E = \Delta_{r_i} V(r_1, ..., r_i) \tag{2.3}$$

The atomic force can be evaluated with Eq 2.1, derivation of acceleration and atomic potential is found using Eq 2.2 and the mass of atom is known.

$$a = \frac{dv}{dt} \rightarrow v(t) = at + v_0 \tag{2.4}$$

$$v = \frac{dx}{dt} \rightarrow x(t) = vt + x_0 = \frac{1}{2}at^2 + v_0 t + x_0 \tag{2.5}$$

Acceleration is found by determining the position and velocity and expansion of Taylor Series is applied as given Eq 2.6 to calculate the equation as the function of time. $O(t^4)$ represents the local truncation error parameter of the fourth order of time step.

$$x(t) = x_0 + v_0 t + a_0 \frac{t^2}{2} + \dot{a_0} \frac{t^3}{3!} + O(t^4) \tag{2.6}$$

$$x(t + \Delta t) = x_0 + v(t)\Delta t + \frac{F(t)}{m}\frac{t^2}{2} + \frac{\dot{F}(t)}{m}\frac{t^3}{3!} + O(t^4) \tag{2.7}$$

Velocity and acceleration are calculated using Eq 2.7 according to time step.

The Verlet Algorithm is most common time integration algorithm in molecular dynamics which is based on Taylor series os expansion according to time step. The Verlet Algorithm is all-round owing to its accuracy, stability and simplicity. Verlet algorithm consists of two Taylor series for the positions x(t). The first Taylor series represents the position of particles forward in time as follow:

$$x(t + \Delta t) = x(t) + v(t)\Delta t + \frac{1}{2}a(t)\Delta t^2 + \frac{1}{6}b(t)\Delta t^3 + O(t^4) \tag{2.8}$$

Likewise, the second Taylor series represents the position of particles backward in time as follow:

$$x(t - \Delta t) = x(t) - v(t)\Delta t + \frac{1}{2}a(t)\Delta t^2 - \frac{1}{6}b(t)\Delta t^3 + O(t^4) \tag{2.9}$$

x(t) stands for position of the particles, v(t) stands for velocity of the particles, a(t) stands for the acceleration of the particles, b(t) stands for the third derivative of the position and $O(\Delta t^4)$ corresponds to the truncation error in both of Taylor series equation.

The primary form of Verlet Algorithm is procured by sum of the Eqs 2.8 and 2.9 as follows:

$$x(t + \Delta t) = 2x(t) - x(t - \Delta t) + a(t)\Delta t^2 + O(t^4) \tag{2.10}$$

Velocity and acceleration of particles can be calculated as follows:

$$a(t) = \frac{x(t+\Delta t) - x(t-\Delta t)}{2\Delta t} \tag{2.11}$$

$$a(t) = -\frac{1}{m}\Delta V(r(t)) \tag{2.12}$$

The Hamiltonian formulation is used to calculate total energy. Hamiltonian mechanic is prefered rather than Lagrangian mechanic in MD simulations. There are a difference between these calculation methods. The Lagranian mechanics depends on the differences of potential and kinetic energies whereas The Hamilton mechanics depends on the summation of these energies as follows:

$$L = K - U \tag{2.13}$$

$$H = K + U \tag{2.14}$$

Definition of potential energy is given by:

$$U(r) = \sum_{i}^{N} U(r_1, ..., r_i) = U_{Bonded} + U_{Non-bonded} \tag{2.15}$$

Definition of kinetic energy is given by:

$$K = \frac{3}{2}Nk_BT = \sum_{i}^{N}\frac{1}{2}m_i(v_i)^2 = \sum_{i}^{N}\frac{(p_i)^2}{2m_i} \tag{2.16}$$

Derivative of The Hamiltonian according to time is equal zero, $\partial H/\partial t = 0$. As a conclusion, atomic coordinates and momenta can be obtained from the initial conditions and potential functions.

2.1 Statistical Ensembles

MD supplies information about microscobic state of the system including atomic positions, velocities and accelerations. Statistical mechanics links up microscopic state of the system with observable macroscopic data such as pressure, temperature or energy condition. Temperature, pressure, density, total energy and number of particles represent thermodynamic state os the system and are controlled by statistical ensembles. Main statistical ensembles can be given as follows:

- Microcanonical ensemble (NVE): The system is controlled by keeping constant number of particles (N), volume (V) and energy (E).

- Canonical ensemble (NVT): Canonical ensemle is used to monitor probility scatter of the macroscopic states of the system in statistical mechanics. The system is controlled by keeping constant number of particles (N), volume (V) and temperature (T).

- Isothermal-isobaric ensemble (NPT): The system is controlled by keeping constant number of particles (N), pressure (P) and temperature (T).

- Isoenthalpic-isobaric ensemble (NPH): The system is controlled by keeping constant number of particles (N), pressure (P) and enthalpy (H).

- Grand canonical ensemble (μVT): The system is controlled by keeping constant chemical potential (μ), volume (V) and temperature (T).

2.2 Boundary of Simulation Region

MD simulation begins by distributing the particles to be analyzed into a simulation region. To make this distribution correctly, the bounderies of the region where the simulation takes place must be specified. The boundaries of the region where the simulation actualises are determined by the number of particles and the density of the material being examined at the temperature to be investigated. A rectangular prism or a cube region is selected for simplicity in terms of programming. Once the volume of the simulation region has been determined, the particles are placed in this volume. The number of particles that can be examined in a simulation program is limited to the performence of the computer. However, even today's advanced computers, it is not easy to examine the amount of particle that is encountered in daily life. If the number of particles examined is not very large, a problem of staying on the boundary surfaces of most of the particles arises. When such a system is examined, the behaviour under the influence of the boundaries of the material itself are examined. Thus, periodic boundary conditions are used to remove this situation.

As seen in Figure 2.1, periodic boundary conditions are basically a replication of the simulation region. The same simulation region is placed around the surfaces of the existing region. In the surrounding areas, there are images of the particles in the current simulation region. When a particle is seperated from the current simulation region, the image of that particle enters from the opposite side. In this way, the number of

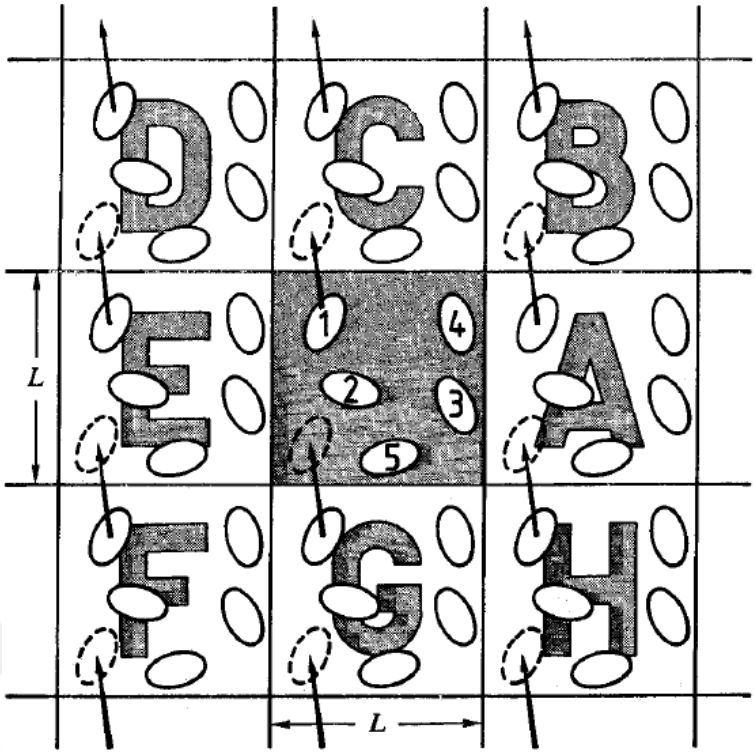

Figure 2.1 : Schematic illustration of periodic boundary conditions [14].

particles in the simulation region is always constant. This method is frequently used in MD applications.

2.3 Interatomic Potentials

Interatomic potentials which are used to describe interactions of atoms is a significant parameter to evalute desired results correctly. The most general form of an interatomic potential is given as follows:

$$U(r_1, r_2, ..., r_N) = \sum_i W_1(r_i) + \sum_{i,j>i} W_2(r_i, r_j) + \sum_{i,j>i,k>j} W_3(r_i, r_j, r_k) \tag{2.17}$$

In Eq 2.17, W_1 represents a one body potential which means external force or external boundary conditions for particles in the simulation region such as field of gravition or a wall function respectivelly. W_2 defines a two body potential which depends interatomic potential on the distances (r_{ij}) between pairs of atoms (r_i and r_j) in the atomic system. W_3 describes as three body potential and when order of potential increases, potentials add energy into the total potential energy of the system.

There are lots of pairwise interactions. However, Lennard-Jones potential (LJ), embedded atom method (EAM) and adaptive intermolecular reactive emprical

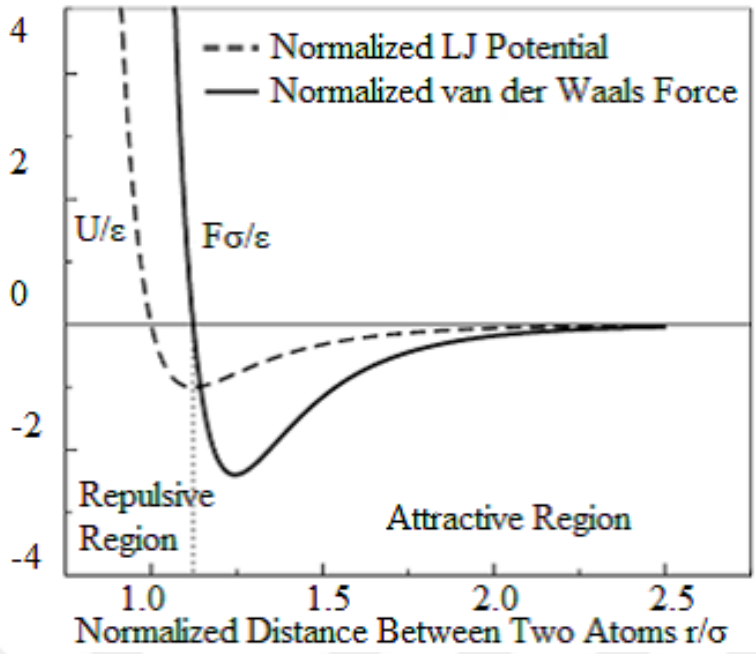

Figure 2.2 : LJ Potential and Van der Waals Force versus Distance [15].

bond-order potential (AIREBO) are used in this thesis. Thus, these potentials will be emphasized in this thesis.

Lennard-Jones (LJ) potential is used Van der Walls system and is most well-known potential. It is also known as 12-6 potential owing to its formulation as given Eq 2.18.

$$u_{LJ}(r_{ij}) = 4\varepsilon\left[\left(\frac{\sigma}{r_{ij}}\right)^{12} - \left(\frac{\sigma}{r_{ij}}\right)^{6}\right] \tag{2.18}$$

LJ depends on two parameter such as ε and σ that used for arranging magnitude of energy between particles and change of atomic distance, respectively. Characteristic of LJ potential is given in Figure 2.2.

Embedded atom method (EAM) is a semi-emprical pairwise interaction which interests each atom in simulation box and is embeded in a host lattice surroundings [81]. EAM is mostly used for metal atoms.

$$E_i = F_\alpha\left(\sum_{i\neq j}\rho_\beta(r_{ij})\right) + \frac{1}{2}\sum_{i\neq j}\varphi_{\beta\alpha}r_{ij} \tag{2.19}$$

In Eq 2.19, r_{ij} is distance between atoms i and j, $\varphi_{\beta\alpha}$ is a function of pairwise potential, ρ_β is the donation of the electron charge density from atom j of type β at the location of atom i. F represent an embedded function which evaluates the motion energy between atoms i and α.

Stuart et. al. [82] developed Adaptive Intermolecular Reactive Emprical Bond-Order (AIREBO) Potential that is investigated interactions between Carbon and Hydrogen. This potential is obtained that is enhanced properties of Reactive Emprical Bond-Order (REBO) [83] potential and include non-bonding atomic interactions. AIREBO also includes long range atomic interactions andf torsional terms in addition to REBO.

$$E_{AIREBO} = \sum_{i} \sum_{i \neq j} \left[E_{ij}^{REBO} + E_{ij}^{LJ} + \sum_{k \neq i,j} \sum_{l \neq i,j,k} E_{kijl}^{TORSION} \right] \tag{2.20}$$

where the total interaction energy is E_{AIREBO}, interaction of REBO is E_{ij}^{REBO}, LJ interaction is E_{ij}^{LJ}, interactions of torsion is $E_{kijl}^{TORSION}$.

3. MODELLING AND SIMULATION

3.1 Formation of Np Metals Reinforced with Carbon Based Nanomaterials

Np metal reinforced with carbon based nanomaterials is modelled two different part that include structure of np metal and network of carbon based nanomaterials. Firstly, structure of np is constituted that contains four stage. The first stage is included that cretaed a point cloud quasi-randomly according to certain parameters. In the second stage, line segments are obtained using the point cloud with Voronoi tesellation (VT) technique, as seen in Figure 3.1. VT have very wide range application field such as biology [84], materials science [85, 86], geography [87], astronomy [88]. VT is a kind of stochastic patterns in nature [89]. The cells that are obtained by VT methods include the number of cells, the areas of cells, the lengths of edges. Coordinate information of these edges which are called line segments are required to generate the ligaments.

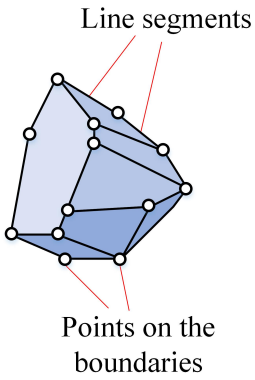

Figure 3.1 : A representative Voronoi cell [16].

In the next stage, the line segments are transformed into volumetric regions to achieve np structure. As shown in Figure 3.2, firstly, main spheres are located at end points of line segments and then, linearly decreasing diameter of spheres are located according to lengths of lines. This process is applied all line segments and obtained volumetric structure. And then, those volumetric structure are filled with FCC (Face Centered Cubic) gold atoms. Therefore, np atomic structure is obtained [39]. In this thesis, FCC gold atoms are selected for metal part of models, inasmuch as np gold is an ideal

structure for several important properties such as tunable and uniform ligament size, dealloying easily, and not form of an oxide layer [31].

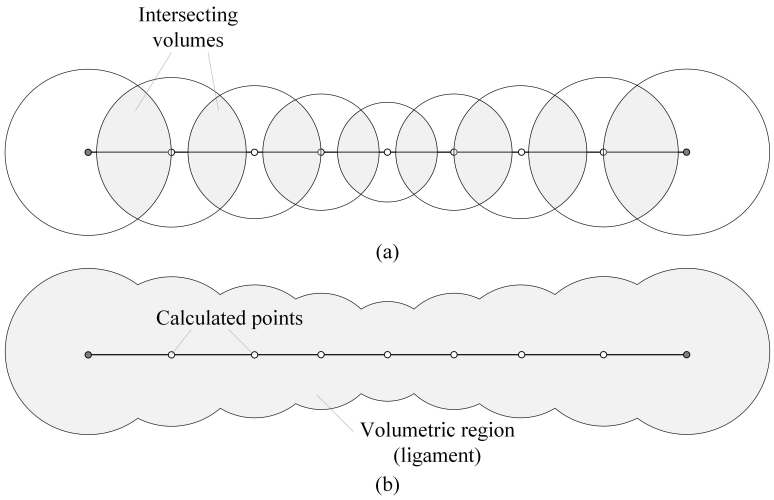

Figure 3.2 : Formation of ligaments [16].

Secondly, network of carbon based nanomaterials is done by taking into account cellular voids. This operation is contained three stage. Point cloud is genetared according to volume of np structure and size of cabon based nanomaterials that is the first stage. Then, cabon based nanomaterials are located to this points according to different orientation. The final stage of distribution of cabon based nanomaterials is that volumetric regions of np structure are removed from volume of cabon based nanomaterials. Finally, two structures are combined and np gold reinforced with cabon based nanomaterials are obtained. Dimensions of np structure is $310\dot{A} \times 310\dot{A} \times 310\dot{A}$ and lattice units of gold atom is $4.080\dot{A}$ [90]. Porosity ratio of np gold is % 56.

As seen in Figure 3.3, first step (1) represents locating carbon based nanomaterials to point cloud, second step (2) shows that volume of carbon based nanomaterials is deleted according to np structure, and third step (3) is combination of np structure and network of carbon based nanomaterials.

In this study, we aim to examine effect of cabon based nanomaterials on mechanical properties. Thus, we used nanoribbons, CNTs, and fullerenes provided that carbon numbers are fixed and np structure is same for all models as well. Length and width of nanoribbons are 1.5 nm and 0.5 nm, respectively. Nanoribbons are used three layer and every layers consists of 56 carbon atoms. This structures are located to point cloud with three different orientation that x, y, and z directions. CNTs and fullerenes are defected randomly. Length of defected CNTs is 1 nm and every CNT is include 90 carbon

atoms. They are oriented according to x, y, z direction and are located to point cloud. Defected C60 fullerenes are used for nanomomposite structures with fullerenes and that contain 50 carbon atoms. Number of point in point cloud is different for different structures in order to keep constant number of carbon atoms every nanocomposite structures. Every models approximately consist of 365 thousand carbon atoms and 773 thousand gold atoms.

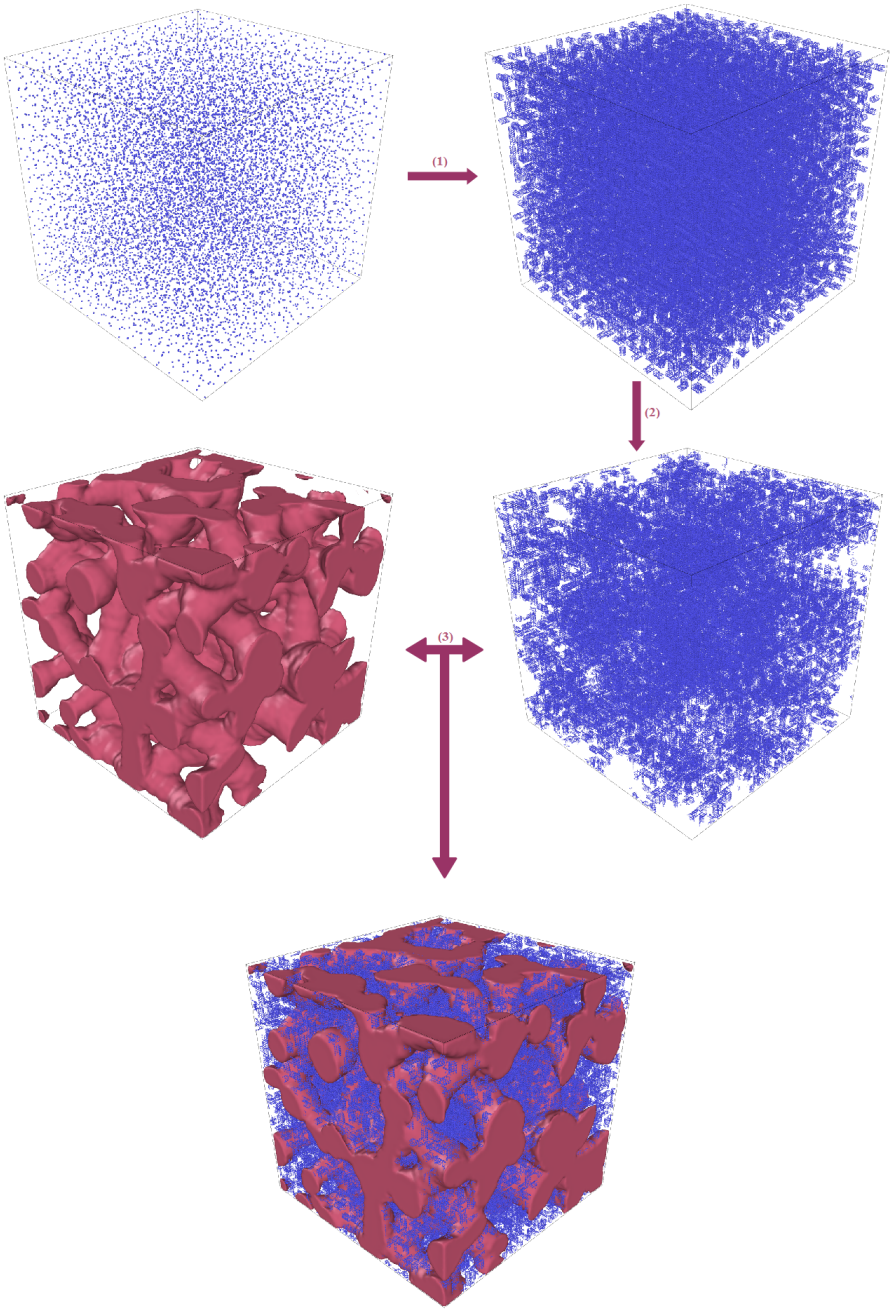

Figure 3.3 : Formation of nanoporous metals reinforced with carbon based nanomaterial.

3.2 Simulation Techniques

The models are simulated by using the open source code LAMMPS [91, 92] (Large-scale Atomic Molecular Massively Parallel Simulator) to examine the mechanical behaviour under uniaxial compressive stress. The interactions between the metal atoms are modeled by using embedded atomic method (EAM) potantial [90] while adaptive intermolecular reactive empirical bond order (AIREBO) potential [93] is employed for the interaction of carbon atoms. Moreover, atomic interactions between the metal and carbon atoms are represented by Lennard-Jones potential [94] with appropriate parameters. All three directions are applied periodic boundary conditions and time step is set as 0.001 ps.

Equilibration is comprise of two stage. Firstly, nanostructures were equilibrated to ensure bond formation with NVT ensemble for 40 ps at 600 K. Secondly, nanostructures were equilibrated to equal zero for interior volume of nanostructures with NPT ensemble for 100 ps at 300 K. Afterwards they were deformed with 0.001 ps^{-1} strain rate under uniaxial compression when NVE ensemble was applied at 300 K throughout simulations.

Thanks to defected structure, bonds are established and fullerenes preserves shape partially (Figure 3.4). However, bonds are not intense owing to low number of open ends (Figure 3.5).

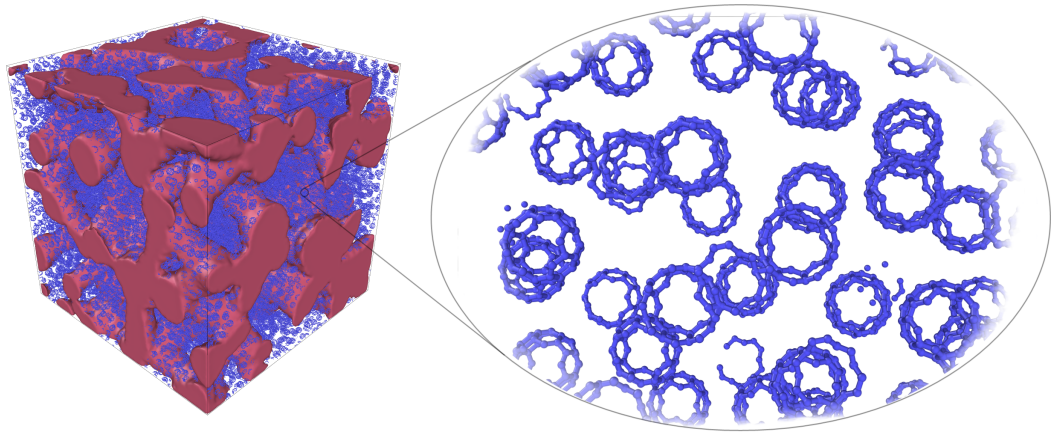

Figure 3.4 : Fullerenes ensembles before thermalization.

Shape of CNTs are collapse under thermalization because of defected structure and open-ended (Figure 3.6). However, tendency to bond increases (Figure 3.7).

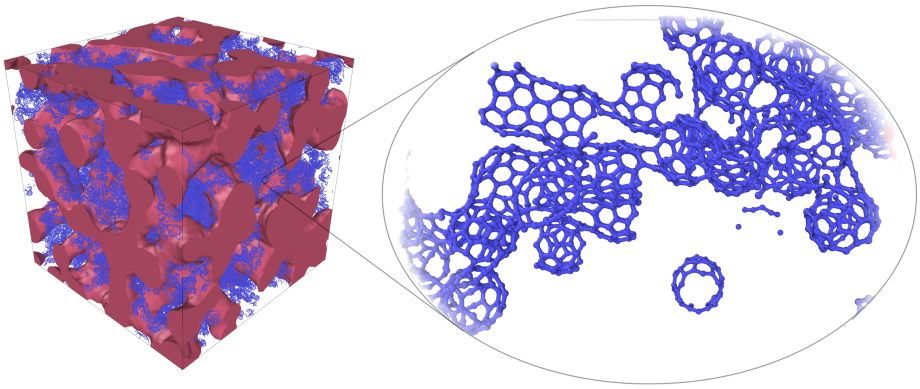

Figure 3.5 : Bond formation between fullerenes after thermalization.

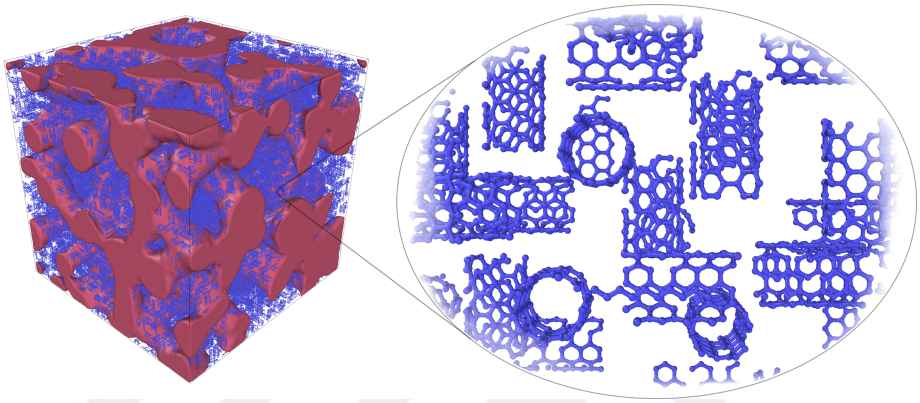

Figure 3.6 : CNTs ensembles before thermalization.

Model with nanoribbons have most open-ended carbon structure in all models (Figure 3.8). Thus, tendency to bond is high (Figure 3.9).

Carbon based nanomaterials approach each other and tend to bond under the effect of tempreture. Thus, a network occurs with bond formation. This network spreads all cellular voids and connect each carbon based nanomaterials.

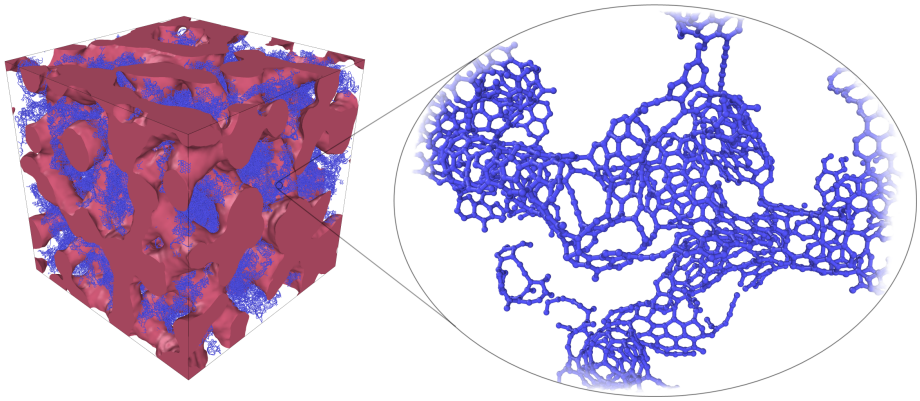

Figure 3.7 : Bond formation between CNTs after thermalization.

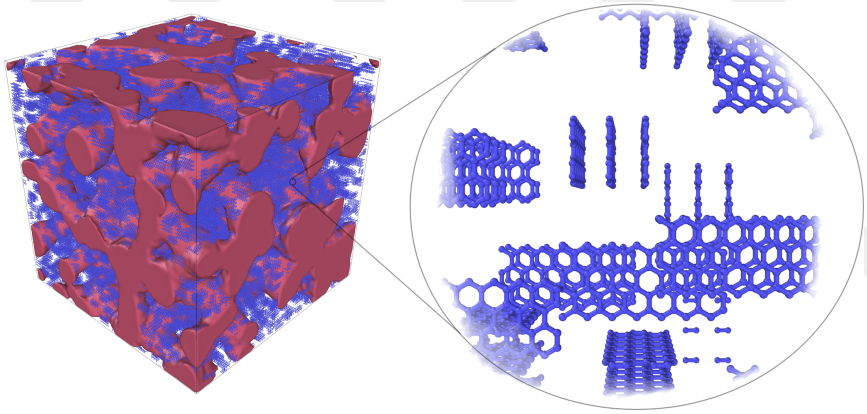

Figure 3.8 : Nanoribbons ensembles before thermalization.

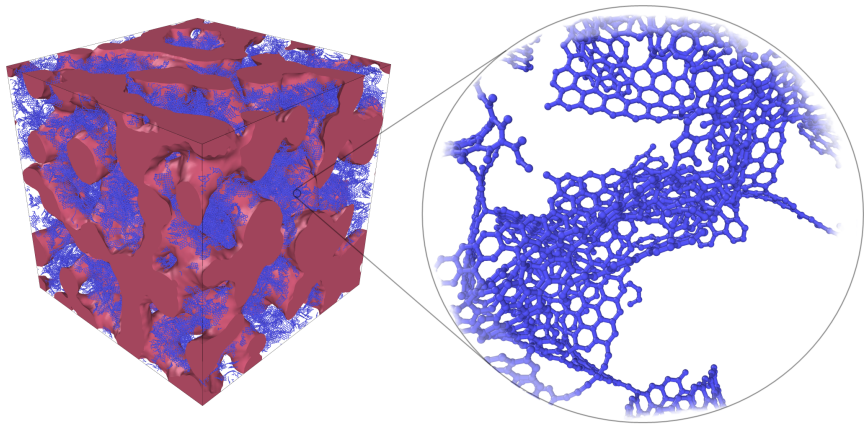

Figure 3.9 : Bond formation between nanoribbons after thermalization.

4. RESULTS AND DISCUSSIONS

4.1 Tensile Response

Uniaxial tensile test are obtained stress-strain curves which gives information as to mechanical properties of materials such as Young's modulus, yield strength, ultimate tensile strength, and fracture strength. Figure 4.1 exhibits a specimen of uniaxial tensile test and stress-strain curve that include important parameter of tensile test. As seen Figure 4.1, stress-strain curve includes two section which is elastic and plastic strain. Plastic strain is divided into uniform and non-uniform plastic deformation in itself.

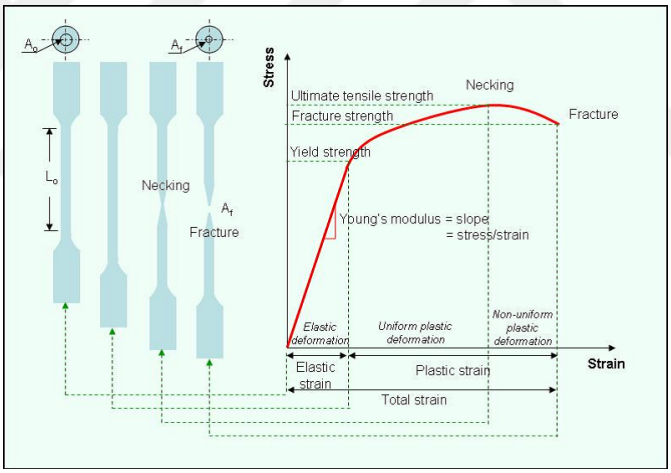

Figure 4.1 : Stress-Strain Relationship under Uniaxial Tensile [17]

Virial Stress Theorem is used for calculation of atomic stresses owing to suitable for MD simulation codes and periodic boundary conditions [95]. The atomic stresses are calculated according to external pressure which is equal to internal principle stress components $(\sigma_{xx}, \sigma_{yy}, and, \sigma_{zz})$ and shear stress components $(\sigma_{xy}, \sigma_{yz}, and, \sigma_{xz})$ is equal to zero at equalibrium owing to hydrostatic pressure [96].

$$P = \frac{1}{3}(\sigma_{xx} + \sigma_{yy} + \sigma_{zz}) \tag{4.1}$$

$$\sigma_{xx} = \sigma_{yy} = \sigma_{zz} \tag{4.2}$$

$$\sigma_{xy} = \sigma_{yz} = \sigma_{xz} = 0 \tag{4.3}$$

This pressure depends on virial theorem and calculated as follow [95]:

$$P = \frac{Nk_BT}{V} + \frac{\langle W \rangle}{3V} \tag{4.4}$$

where N is number of interacting atoms, k_B is Boltzmann's constant, V is volume of simulation box, W is internal virial which depends on atom positions (r_i) and and interacting force (F_i) between atoms, as given in Equation 4.5.

$$W(r^N) = \sum_{i=1}^{N} r_i \cdot F_i \tag{4.5}$$

Figure 4.2 shows the deformation under tensile stress of models using different types of carbon based nanomaterials (CBNMs). When we examine stress-strain curve for uniaxial tensile test. If elastic region of stress-strain curve is investigated, young modulus does not increase too much for all models. Because, carbon based nanomaterials are not effected under uniaxal tensile stress for elastic region. However, differences between all models reveals region of uniform plastic deformation. Ultimate tensile stress is ordered from the highest to the lowest as np Au with CNTs, np Au with nanoribbons, np Au with fullerenes and np Au, respectively. Ultimate stress of np Au that is 0.45 GPa can be approximately increased to 0.55 GPa, 0.54 GPa and, 0.50 GPa by using CNTs, nanoribbons and, fullerenes, respectively.

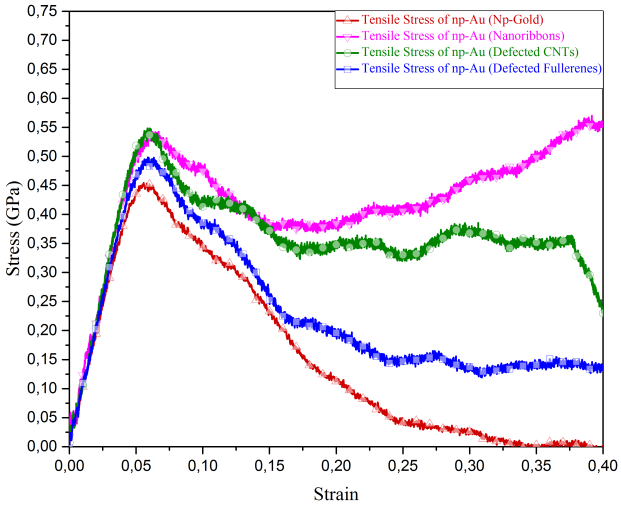

Figure 4.2 : Results of tensile stress for all models

Effects of CBNMs appear after 5% strain owing to influence of tensile stress do not reach carbon atoms. After yield point that is almost equal for all structures is observed

distinct differences due to the fact that CBNMs come into play in tensile stress. Main differences for all models is seen in non-uniform plastic deformation region because of behaviour of network of CBNMs. When we compare with Figure 4.3 and Figure 4.2, strength of carbon bonds of np gold with nanoribbons (NPGwNRs) is stronger than other models. Since, tendency of bonding of nanoribbons are very high due to having open-endend all edges of nanoribbons.In addition, although np Au ruptures, np Au with nanoribbons have a second peak point owing to stiffness and homogen distribution of composed carbon network. Nanoribbons expand filamentlike. After ligaments of np Au split and new voids occur, nanoribbons are spread to the voids. The expansion increases as the voids increases owing to high tendency of bonding for nanoribbons. Thus, a complex and durable network appears. Behaviour of transverse expansion is dominant rather than longitudinal elongation. Stress-strain curve of np gold with CNTs (NPGwCNTs) have trough due to abrubt delaceration of CNTs network as seen in Figure 4.3-b(5). Tensile response of NPGwCNTs is higher than np gold with fullerenes (NPGwFs). Behaviour of NPGwFs resembles offset curve of np gold. Behaviour of fullerenes network is stable and their bonds are not strong to keep interaction of carbon atoms. CBNMs influence in terms of increasing strain failure for all models. Even if np structure ruptures, network of CBNMs keep on carrying load.

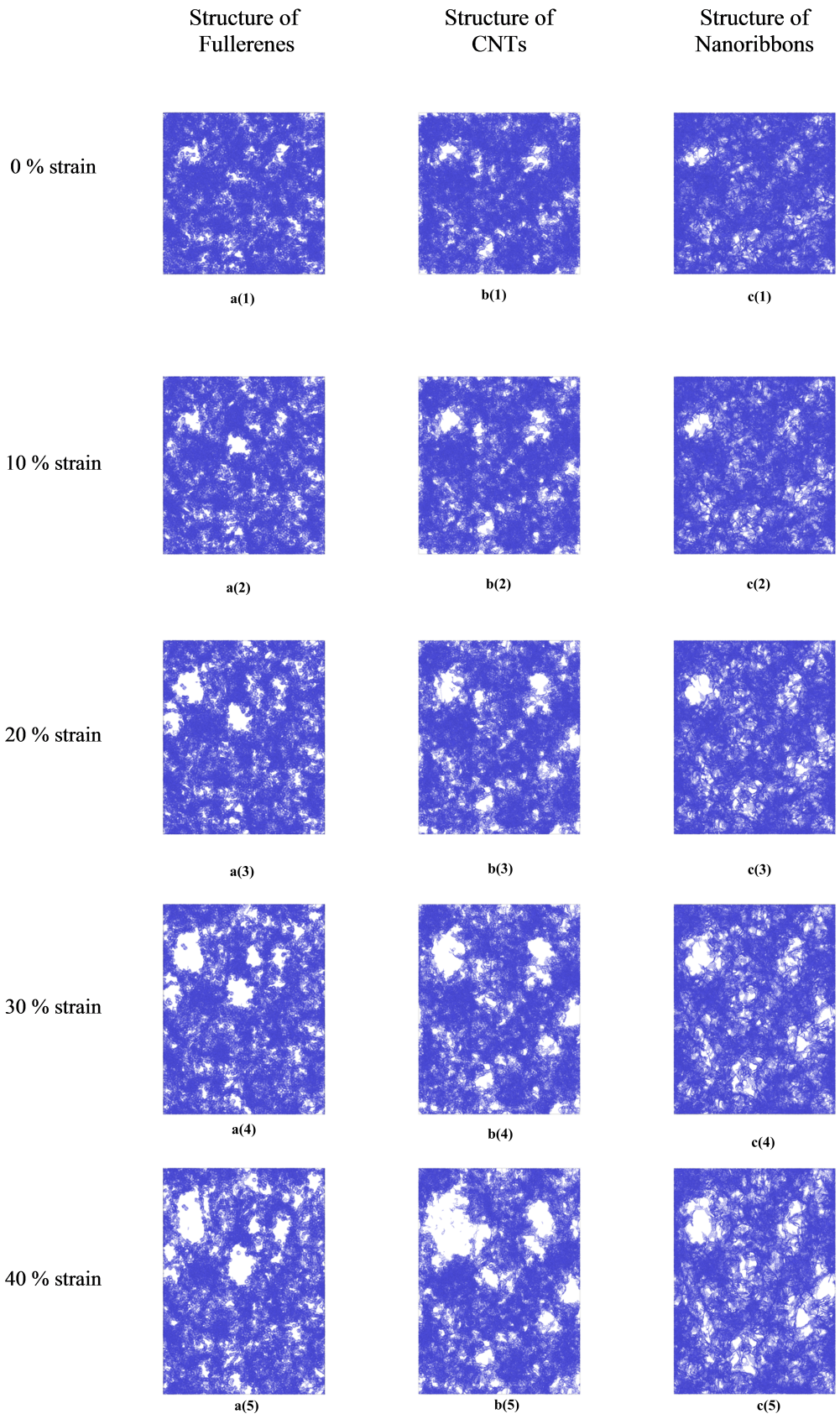

Figure 4.3 : yz plane illustration of all carbon based nanomaterials under tensile stress

When we investigate relationship between formed bonds and tensile response for all models, change of tensile stress is associated with number of bonds (see Figure 4.4). Initial bond number of NPGwNRs after welding and equilibration is maximum in all models. If the curves of bond number plunge to below zero, it means that the earlier bonds or new bonds collapse. Tensile response of NPGwFs and NPGwCNT is similar in terms of bond decrease. Namely, tensile stress decreases as number of bonds decreases. However, vice versa for NPGwNRs owing to durability of new bond combinations.

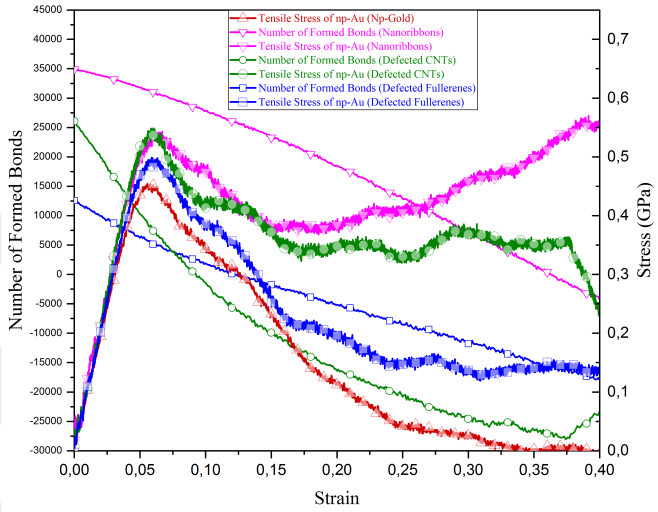

Figure 4.4 : Relations of tensile stress with number of formed bonds for all models

The common neighbor analysis (CNA) defines defects under deformation. There are four type atoms in different colors: red for FCC atoms, green for body-centered-cubic (BCC) atoms, yellow for hexagonal-close-packed (HCP) atoms, and blue for non-12-coordinated atoms. Figure 4.6 and Figure 4.7 is demonstrated CNA results with applied strain for all models. Fraction of HCP atoms gives information about plastic deformation under loading. Figure 4.5 examine four division. First division includes between initial points and yield point. The stress increases linearly during loading in this region. Hovever, the fraction of HCP is constant due to the that fact motion of dislocation is not active. Second division contains between yield point and ultimate stress point. The stacking faults increase while strain increases in this region. Thus, the fraction of HCP atoms increase. Region of between ultimate stress point and fracture point represent third division. Large deformation and rupture of ligaments observe in this region. Last region is fourth division. The fraction of HCP is nearly constant even if the strain increases. Our results demonsrate that effects of cabon

based nanomaterials is not significant because of not having direct inflence to lattice structure.

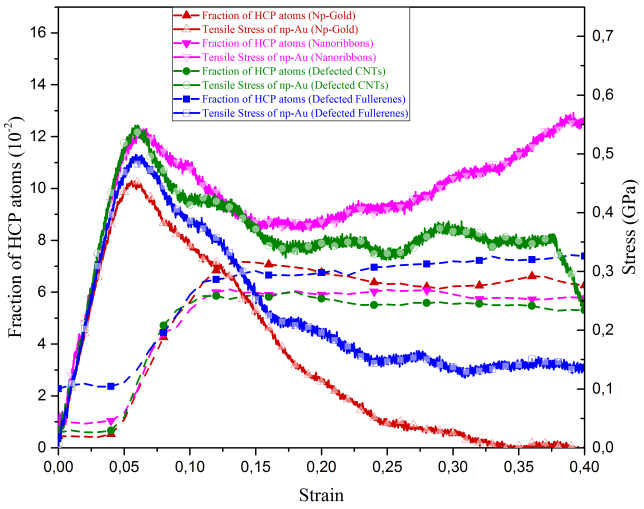

Figure 4.5 : Results of tensile stress with fraction of HCP for all models

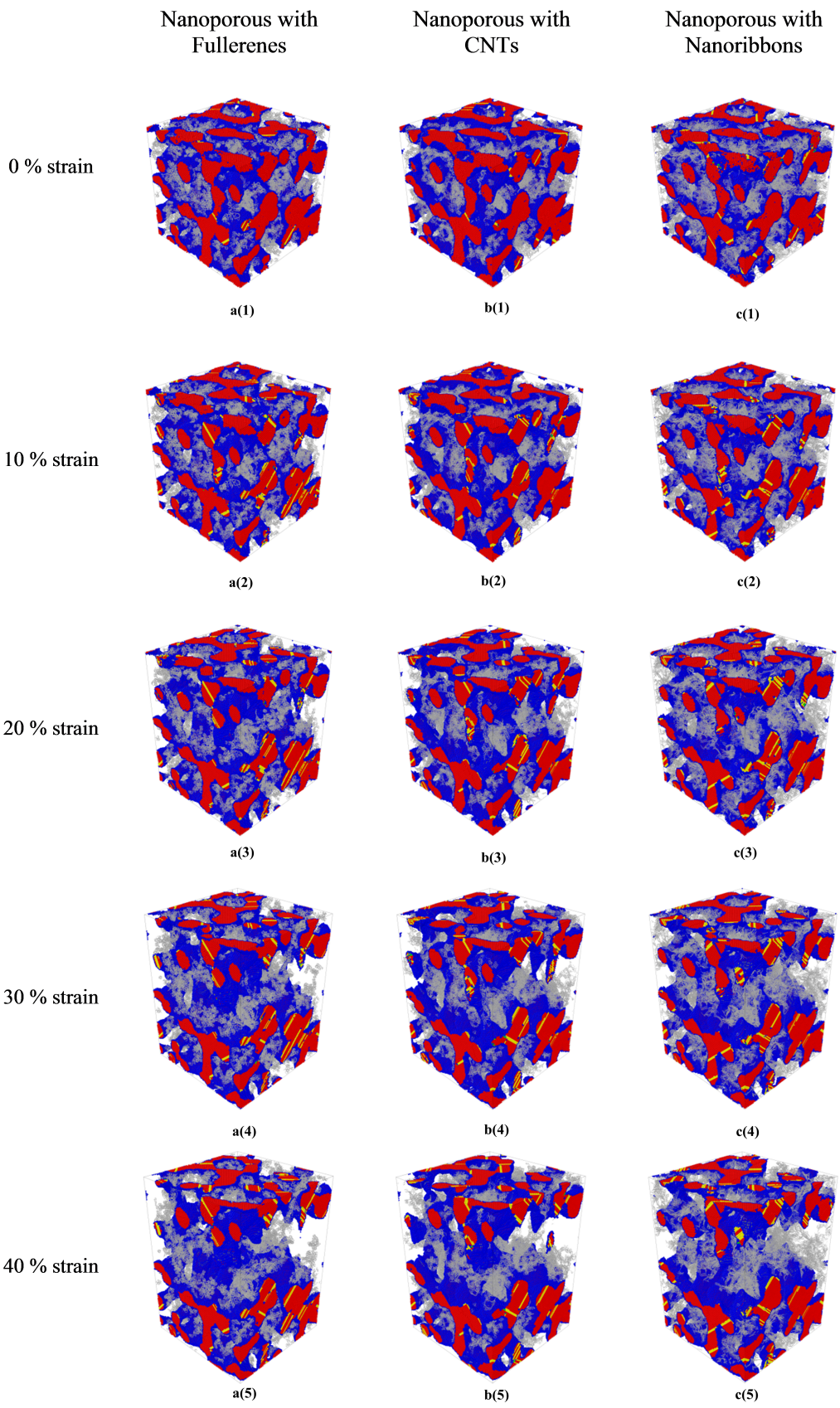

Figure 4.6 : Perspective illustration of all models under tensile stress

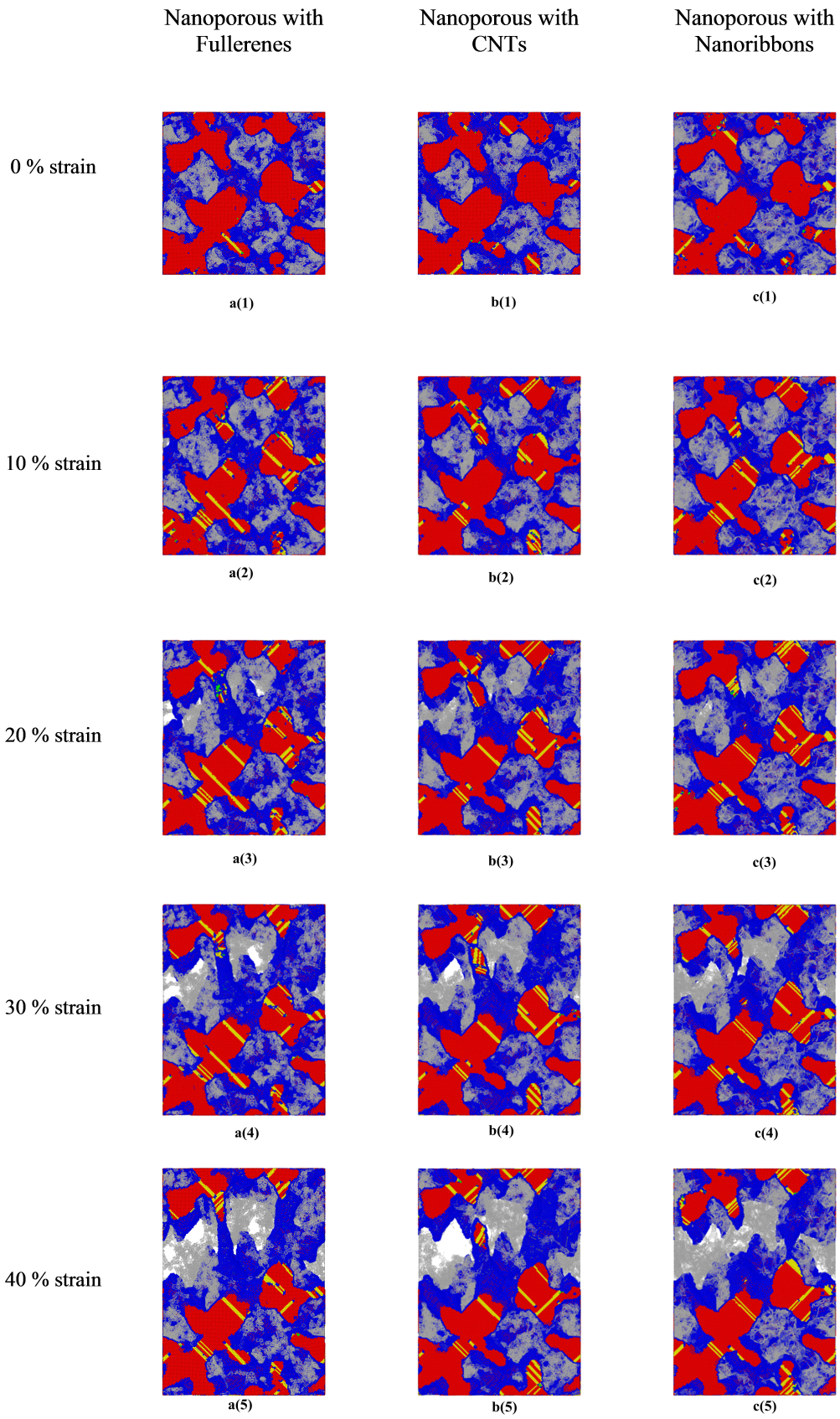

Figure 4.7 : yz plane illustration of all models under tensile stress

4.2 Compressive Response

The graph of compression stress is divided into 3 (three) regions, as seen Figure 1.10. The first part of the graph refers to the linear elastic region, the second region refers to plateau (namely the work hardening region or plastic yielding) region and the last region refers to the densification region. When we apply compression force to the same models, as shown in Figure 4.8, all the models in the elastic region show the same characteristics and when the load is removed, the structure returns to its original state. Deformation occurs without increasing density as the loading increases in the second region and the cells start to collapse. When the similar stress value are obtained for the models that is reinforced with carbon based nanomaterials for this region, less tress values are obtained in the model of nanoporous gold than other models. Since, carbon based nanomaterials support the cells during compression and build up resistance against collapse. In the last region, it is called densification region because of most of cells collopse. Resistance of all models increases rapidly. The main difference between the models is seen here.

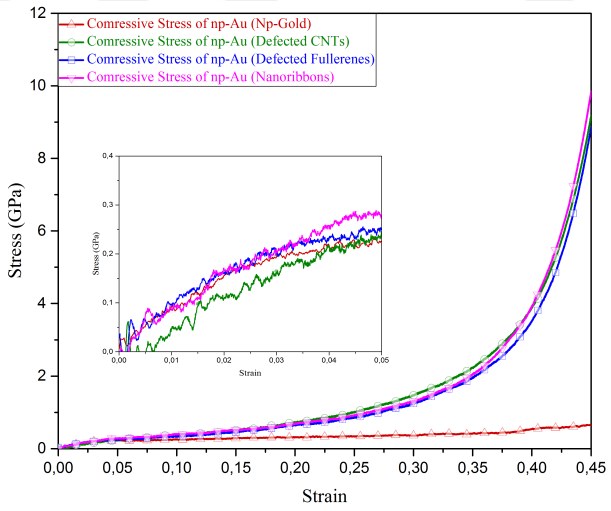

Figure 4.8 : Results of compressive stress for all models

The carbon networks for all models act almost simlilar in comressive loading, as seen in Figure 4.9. Since, amount of carbon is nearly same for all models with carbon based nanomaterials. The main difference emerges in the densification region slightly.

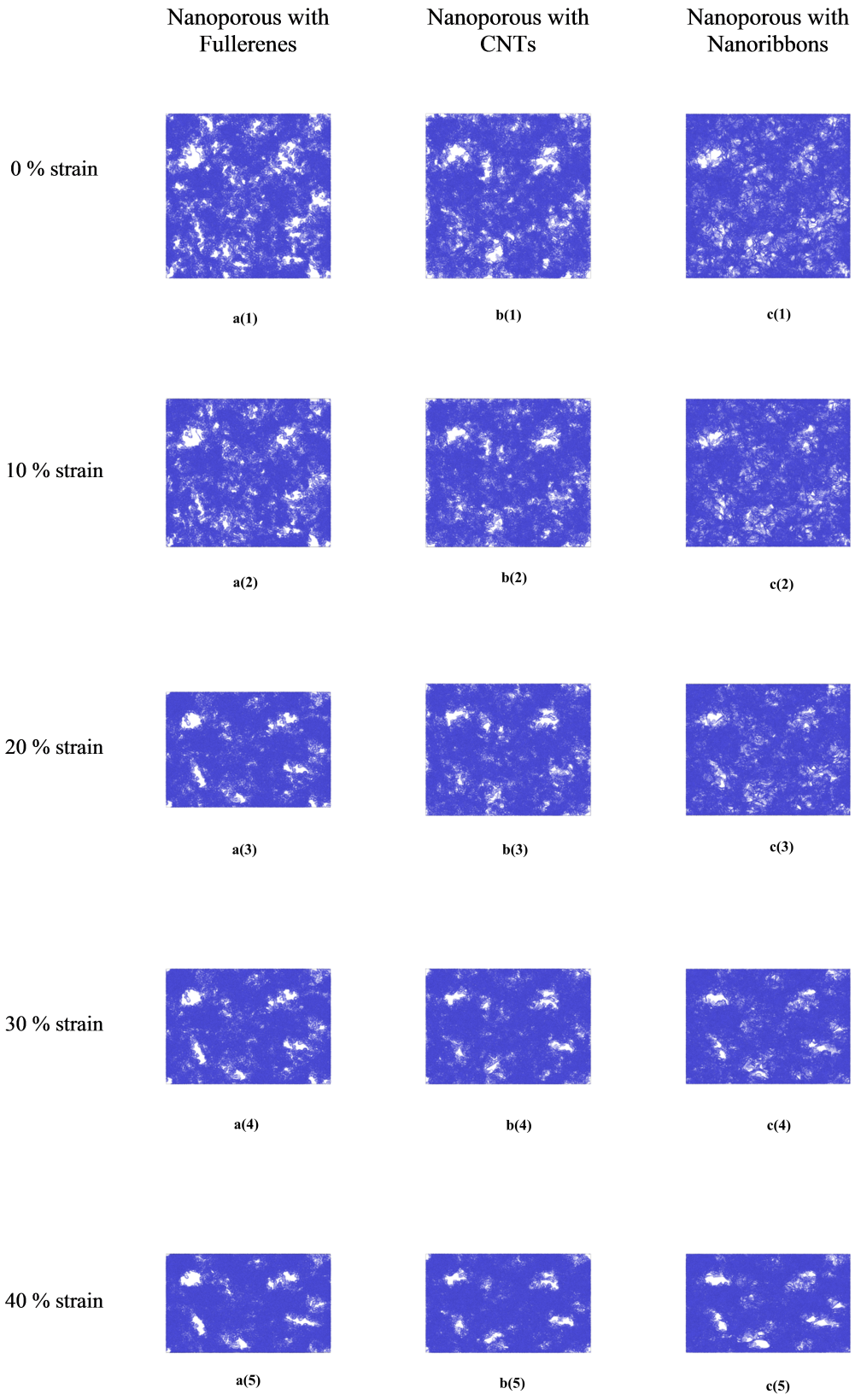

Figure 4.9 : yz plane illustration of all carbon based nanomaterials under compressive stress

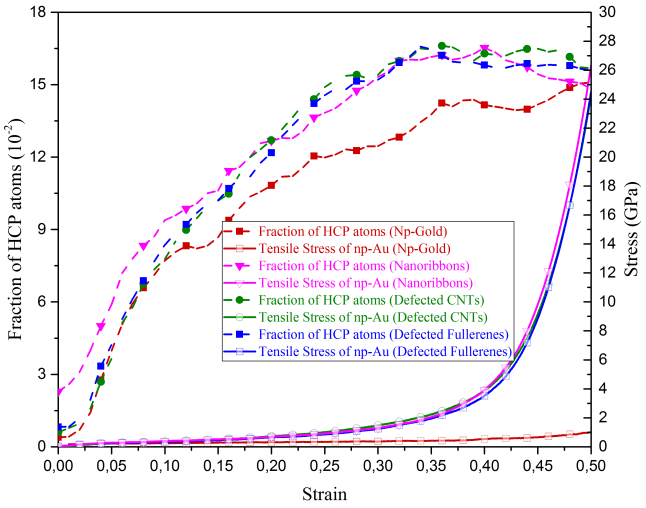

Figure 4.10 : Results of compressive stress with fraction of HCP for all models

If we examine all models in terms of CNA, difference arises in the densification region between np Au and np Au reinforced with carbon based nanomaterials, as seen in Figure 4.10. There is almost no difference between the models with carbon-containing in point of HCP atoms. Carbon atoms affect amount of HCP atoms owing to atomic interactions.

4.3 Effects of Strain Rate

Strain rate is an important parameter for understanding of materials behaviour under loading. If the strain rate increases and the strength of a material increases, the resistance of the material to plastic deformation increases. Namely, it's getting harder to change the plastic strain. When Figure 4.13 is investigated in terms of tensile loading, we can report that if strain rate is increases, toughness is incerses. However, Young's module and yield strength of structures are not changed. When the results of compressive loading is examined in Figure 4.13, we can obtain that there is no influence for compressive loading in terms of strain rate. All structures were deformed under uniaxial tensile and compressive loading at 300 K at three different uniform strain rate that are 0.001 ps^{-1}, 0.002 ps^{-1}, 0.004 ps^{-1}.

Firstly, we examine effect of strain rate in terms of tensile response. In figure 4.13-a(1) represents NPGwFs under different strain rate and we obtain that if strain rate increases toughness, strength of material and ultimate stress increase for this strutucture. In figure 4.13-a(2), namely NPGwCNTs under tensile loading, strain rate of 0.001 ps^{-1}

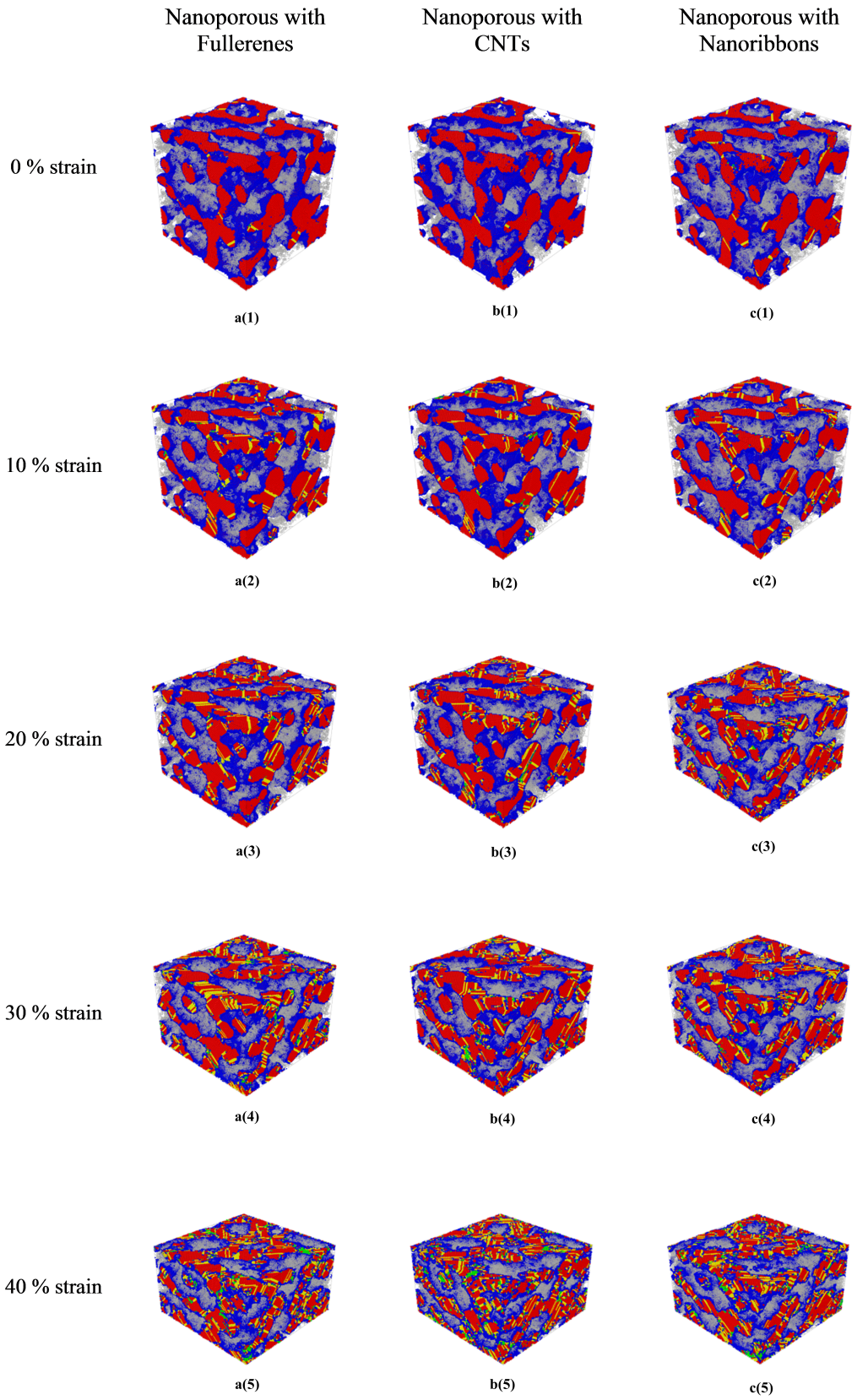

Figure 4.11 : Perspective illustration of all models under compressive stress

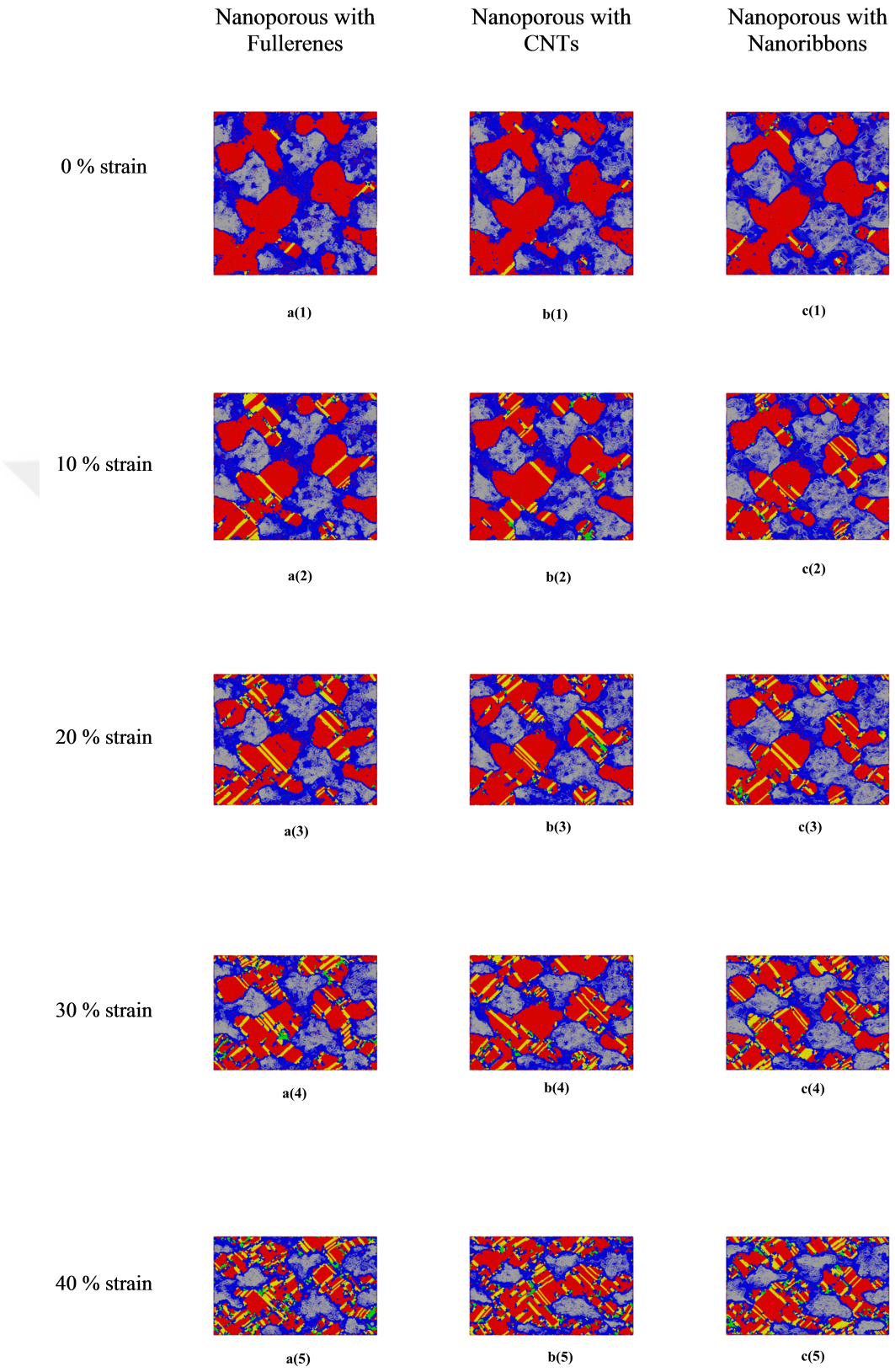

Figure 4.12 : yz plane illustration of all models under compressive stress

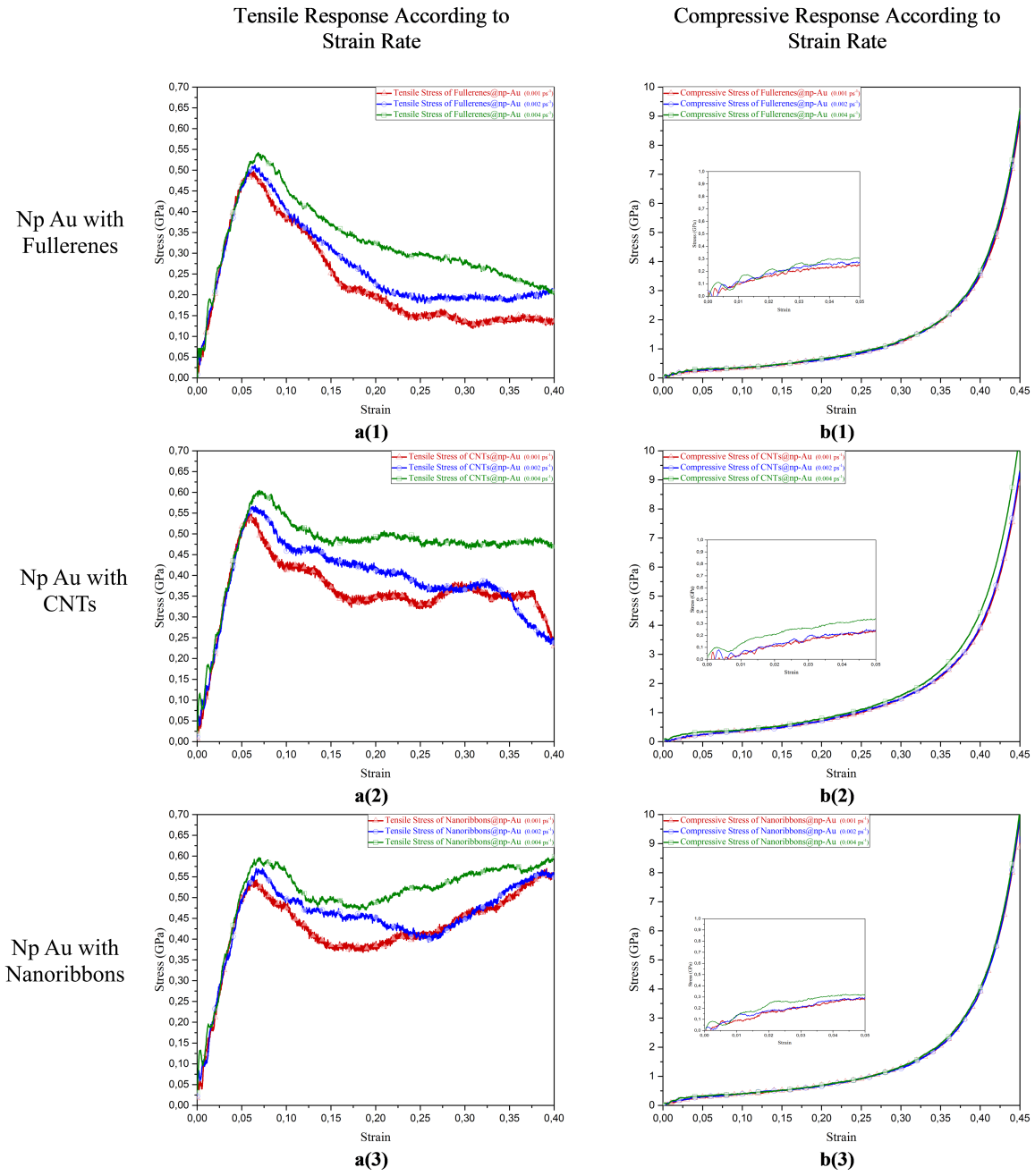

Figure 4.13 : Effects of strain rate for all models

and 0.002 ps^{-1} have similar characteristics in terms of plastic deformation. However, under strain rate of 0.004 ps^{-1} different from response of other strain rate. It means that is strain rate increases, strength of material to plastic deformation increases. Thus, an abrubt drop and a distinct rupture in network of CNTs are not observed. Behaviour of NPGwNRs under various strain rate have familiar effect and same Young's module. However, ultimate stress increases when strain rate increases, as demonstrated in Figure 4.13-a(3).

If we examine the compressive response according to various strain rate, behaviours of all models are almost same at different strain rate. Since, fill rate of cells is nearly same amount of carbon atoms.

5. CONCLUSIONS AND RECOMMENDATIONS

In this thesis, mechanical behavior of np Au reinforced with carbon based nanomaterials are investigated by using MD simulation under uniaxal tensile and compressive loading. Fullerenes, CNTs, and nanoribbons are used as carbon based nanomaterials for nanocomposites. Main idea is to improve mechanical properties of np Au by stuffing the pores of np Au with carbon based nanomaterials. Namely, it is aimed to obtain a novel material by combining np Au and carbon based nanostructures. Three different models that have same amount of carbon are created to investigate effect of carbon based nanomaterials in np au. It was reported that carbon increases strength of np Au both tensile and compressive loading. Yield strength, thoughness and ultimate stress of the structures increase but Young's module of the structures do not change. Compressive strength increases owing to filling of pores. There was no significant difference in terms of CNA both tensile and compressive loading. It was obtained that there was no significant effect under compressive stress in terms of effect of strain rate while there are apparent influence under tensile stress.

For future plans, effect of different tempreture for all models will be investigated under loading. In addition different porosities of np Au with carbon based nanomaterials will be examined. Besides, we are planing to use boron-nitride based nanomaterials instead of carbon based nanomaterials. It is planed to construct to ligaments of np Au carbons network like a spiral. It is possible that different metal are used for main structure. Bonding molecules can be used to connect and wrap metals and carbon atoms.

REFERENCES

[1] **Rao, C.N.R. and Cheetham, A.K.** (2001). Science and technology of nanomaterials: current status and future prospects, *Journal of Materials Chemistry*, *11*, 2887–2894.

[2] **Kalamkarov, A.L.**, **Georgiades, A.V.**, **Rokkam, S.K.**, **Veedu, V.P. and Ghasemi-Nejhad, M.N.** (2006). Analytical and numerical techniques to predict carbon nanotubes properties, *International Journal of Solids and Structures*, *350*, 6832–6854.

[3] **Institute, N.C.**, `https://www.cancer.gov/research/progress/snapshots/nanotechnology`, accessed: 04 11 2014.

[4] **Roco, M.C. and Hersam, C.A.M.M.C.** (2012). Zero-dimensional, one-dimensional, two-dimensional and three-dimensional nanostructured materials for advanced electrochemical energy devices, *Progress in Materials Science*, *57*, 724–803.

[5] **Kırca, M.** (2013). Mechanics of nanomaterials consisted of random networks, *Ph.D. thesis*, Istanbul Technical University.

[6] **Pugh, D.V.**, **Dursun, A. and Corcoran, S.G.** (2003). Formation of nanoporous platinum by selective dissolution of Cu from $Cu_{0.75}Pt_{0.25}$, *Journal of Materials Research*, *18*, 216–221.

[7] **Ngo, B.N.D.**, **Stukowski, A.**, **Mameka, N.**, **Markmann, J.**, **Albe, K. and Weissmüller, J.** (2015). Anomalous compliance and early yielding of nanoporous gold, *Acta Materialia*, *93*, 144–155.

[8] **Gibson, L.J. and Ashby, M.F.**, (1997). Cellular Solids: Structure and Properties, Cambridge University Press, 2. edition.

[9] **Biener, J.**, **Hodge, A.M.**, **Hamza, A.V.**, **Hsing, L.M. and Satcher, J.H.** (2005). Nanoporous Au: A high yield strength material, *Journal of Applied Physics*, *97*, 1–5.

[10] **Biener, J.**, **Hodge, A.M. and Hamza, A.V.** (2007). Deformation Behavior of Nanoporous Metals, *Micro and Nano Mechanical Testing of Materials and Devices*, 118–135.

[11] **Terrones, M.**, **Botello-Mendez, A.R.**, **Compos-Delgado, J.**, **Lopez-Urias, F.**, **Vega-Cantu, Y.I.**, **Rodriguez-Macias, F.J.**, **Elias, A.L.**, **Munoz-Sandoval, E.**, **Cano-Marquez, A.G.**, **Charlier, J.C. and Terrones, H.** (2010). Graphene and graphite nanoribbons: Morphology, properties, synthesis, defects and applications, *Nano Today*, *5*, 351–372.

[12] **Vajtai, R.**, (2013). Springer Handbook of Nanomaterials, Springer, USA, 1. edition.

[13] **Baughman, R.H.**, **Zakhidov, A.A. and de Heer, W.A.** (2002). Carbon nanotubes - the route toward applications, *Science*, *297*, 787–792.

[14] **Allen, M.P. and Tildesley, D.J.**, (1991). Computer simulation of liquids and liquid crystals, Oxford University Press, New York, 2. edition.

[15] **Li, C. and Chou, T.W.** (2003). Elastic moduli of multi-walled carbon nanotubes and the effect of van der Waals forces, *Composites Science and Technology*, *63*, 1517–1524.

[16] **Yıldız, Y.O. and Kırca, M.** (2017). Atomistic simulation of Voronoi-based coated nanoporous metals, *Modelling Simul. Mater. Sci. Eng.*, *25*, 025008.

[17] **Faridmehr, I.**, **Osman, M.H.**, **Nejad, A.B.A.A.F.**, **Hodjati, R. and Azimi, M.** (2014). Correlation and between engineering stress-strain and true stress-strain curve, *American Journal of Civil Engineering and Architecture*, *2*, 53–59.

[18] **Fang, M.**, **Zeisberg, W.**, **Condon, C.**, **Ogryzko, V.**, **Danchin, A. and Mechold, U.** (2009). Degradation of nanoRNA is performed by multiple redundant RNases in Bacillus subtilis, *Nucleic Acids Research*, *37*, 5114–5125.

[19] **Hassan, M.H.A.** (2005). Small things and big changes in the developing world, *Science AAAS*, *309*, 65–66.

[20] **Miyazaki, K. and Islam, N.** (2007). Nanotechnology systems of innovation-An analysis of industry and academia research activities, *Technovation*, *27*, 661–675.

[21] **Whitesides, G.M.** (2005). Nanoscience, Nanotechnology, and Chemistry, *Small*, *2*, 172 –179.

[22] **Virk, H.S.**, (2015). Nanomaterials, Basic Consepts and Applications, Trans Tech Publications, 1. edition.

[23] **Ashby, M.F. and Schodek, P.J.F.D.L.**, (2009). Nanomaterials, Nanotechnologies and Design, Elsevier, 1. edition.

[24] **Gall, K.**, **Diao, J. and Dunn, M.L.** (2004). The strength of Gold Nanowires, *Nano Letters*, *4*, 2431–2436.

[25] **Roco, M.C. and Hersam, C.A.M.M.C.** (2011). Nanotechnology research directions for societal needs in 2020: Summary of international study, *Journal of Nanoparticle Research*, *13*, 897–919.

[26] **Hornyak, G.L.**, **Moore, J.J.**, **Tibbals, H.F. and Dutta, J.**, (2011). Fundamentals of Nanotechnology, CRC Press, 3. edition.

[27] **Zeis, R.**, **Mathur, A.**, **Fritz, G.**, **Lee, J. and Erlebacher, J.** (2007). Platinum-plated nanoporous gold: An efficient, low Pt loading electrocatalyst for PEM fuel cells, *Journal of Power Sources*, *165*, 65–72.

[28] **Lang, X.Y.**, **Yuan, H.T.**, **Iwasa, Y. and Chen, M.W.** (2011). Three-dimensional nanoporous gold for electrochemical supercapacitors, *Scripta Materialia*, *64*, 923–926.

[29] **Detsi, E.**, **Chen, Z.G.**, **Vellinga, W.P.**, **Onck, P.R. and Hosson, J.T.M.D.** (2012). Actuating and Sensing Properties of Nanoporous Gold, *Journal of Nanoscience and Nanotechnology*, *12*, 4951–4955.

[30] **Bonroy, K.**, **Friedt, J.M.**, **Frederix, F.**, **Laureyn, W.**, **Langerock, S.**, **Campitelli, A.**, **Sara, M.**, **Borghs, G.**, **Goddeeris, B. and Declerck, P.** (2004). Realization and characterization of porous gold for increased protein coverage on acoustic sensors, *Analytical Chemistry*, *76*, 4299–4306.

[31] **Biener, J.**, **Hodge, A.M.**, **Hayes, J.R.**, **Volkert, C.A.**, **Zepeda-Ruiz, L.A.**, **Hamza, A.V. and Abraham, F.F.** (2006). Size effects on the mechanical behavior of nanoporous Au, *Nano Letters*, *6*, 2379–2382.

[32] **Balk, T.J.**, **Eberl, C.**, **Sun, Y.**, **Hemker, K.J. and Gianola, D.S.** (2009). Tensile and compressive microspecimen and testing of bulk nanoporous gold, *Journal of Metals*, *61*, 26–31.

[33] **Briot, N.J.**, **Kennerknecht, T.**, **Eberl, C. and Balk, T.J.** (2014). Mechanical properties of bulk single crystalline nanoporous gold investigated by millimetre-scale tension and compression testing, *Philosophical Magazine*, *94*, 847–866.

[34] **Lee, D.**, **Wei, X.**, **Chen, X.**, **Zhao, M.**, **Jun, S.C.**, **Hona, J.**, **Oliver, W.C. and Kysar, J.W.** (2007). Microfabrication and mechanical properties of nanoporous gold at the nanoscale, *Scripta Materialia*, *56*, 437–440.

[35] **Sun, X.Y.**, **Xu, G.K.**, **Li, X.**, **Feng, X.Q. and Gao, H.** (2013). Mechanical properties and scaling laws of nanoporous gold, *Journal of Applied Physics*, *113*, 023505(1–9).

[36] **Crowson, D.A.**, **Farkas, D. and Corcoran, S.G.** (2009). Mechanical stability of nanoporous metals with small ligament sizes, *Scripta Materialia*, *61*, 497–499.

[37] **Rodriguez-Nieva, J.F.**, **Ruestes, C.J.**, **Tang, Y. and Bringa, E.M.** (2014). Atomistic simulation of the mechanical properties of nanoporous gold, *Acta Materialia*, *80*, 67–76.

[38] **Yıldız, Y.O. and Kırca, M.** (2016). Effects of nano-coating on the mechanical behavior of nanoporous metals, *World Acad Sci Eng Technol Int J Mech Mechatronics Eng*, Amsterdam, The Netherlands.

[39] **Yıldız, Y.O. and Kırca, M.** (2017). Atomistic simulation of the mechanical properties of nanoporous gold, *Modelling and Simulation in Materials Science and Engineering*, *25*, 025008(1–21).

[40] **Hakamada, M. and Mabuchi, M.** (2007). Mechanical strength of nanoporous gold fabricated by dealloying, *Scripta Materialia*, *56*, 1003–1006.

[41] **Kroto, H.W.**, **Heath, J.R.**, **O'Brien, S.C.**, **Curl, R.F. and Smalley, R.E.** (1985). C_{60}: Buckminsterfullerene, *Nature*, *318*, 162–163.

[42] **Gao, F.**, **Zhao, G.L.**, **Yang, S. and Spivey, J.J.** (2013). Nitrogen-doped Fullerene as a Potential Catalyst for Hydrogen Fuel Cells Nitrogen-doped Fullerene as a Potential Catalyst for Hydro- gen Fuel Cells, *Journal of The American Chemical Society*, *135*, 3315–3318.

[43] **Oku, T.** (2004). Hydrogen storage in boron nitride and carbon clusters studied by TG/DTA molecular orbital calculations, *Solid State Communications*, 433–440.

[44] **Oku, T. and Narita, I.** (2002). Calculation of H_2 gas storage for boron nitride and carbon nanotubes studied from the cluster calculation, *Physica B: Condensed Matter*, *323*, 216–218.

[45] **Sherigara, B.S.**, **Kutner, W. and D'Souza, F.** (2003). Electrocatalytic properties and sensor applications of fullerenes and carbon nanotubes, *Electroanalysis*, *15*, 753–772.

[46] **Liu, Z.B.**, **Xu, Y.F.**, **Zhang, X.Y.**, **Zhang, X.L.**, **Chen, Y.S. and Tian, J.G.** (2009). Porphyrin and fullerene covalently functionalized graphene hybrid materials with large nonlinear optical properties, *Journal of Physical Chemistry B*, *113*, 9681–9686.

[47] **Foley, S.**, **Crowley, C.**, **Smaihi, M.**, **Bonfils, C.**, **Erlanger, B.F.**, **Seta, P. and Larroque, C.** (2002). Cellular localisation of a water-soluble fullerene derivative, *Biochemical and Biophysical Research Communications*, *294*, 116–119.

[48] **Hirsch, A. and Brettreich, M.**, (2005). Fullerenes: Chemistry and Reactions, Wiley-VCH.

[49] **Wang, Q.** (2009). Torsional instability of carbon nanotubes encapsulating C60 fullerenes, *Carbon*, *47*, 507–512.

[50] **Zuev, V.V.**, **Kostromin, S.V. and Shlykov, A.V.** (2010). The effect of fullerene fillers on the mechanical properties of polymer nanocomposites, *Mechanics of Composite Materials*, *46*, 147–154.

[51] **Barrera, E.V.**, **Sims, J. and Callahan, D.L.** (1995). Development of fullerene-reinforced aluminum, *Journal of Materials Research*, *10*, 366–371.

[52] **Shin, J.**, **Choi, K.**, **Shiko, S.**, **Choi, H. and Bae, D.** (2015). Mechanical damping behavior of Al/C60-fullerene composites with supersaturated Al-C phases, *Composites Part B: Engineering*, *77*, 194–198.

[53] **Brenner, D.W.**, **Harrison, J.A.**, **White, C.T. and Colton, R.J.** (1991). Molecular dynamics simulations of the nanometer-scale mechanical properties of compressed Buckminsterfullerene, *Thin Solid Films*, *206*, 220–223.

[54] **Iijima, S.** (1991). Hellical microtubules of graphitic carbon, *Nature*, *350*, 627–628.

[55] **Dresselhaus, M.S.**, **Dresselhaus, G. and Saito, R.** (1995). Physics of carbon nanotubes, *Carbon*, *33*, 883–891.

[56] **Treacy, M.M.J.**, **Ebbesen, T.W. and Gibson, J.M.** (1996). Exceptionally high Young's modulus observed for individual carbon nanotubes, *Nature*, *381*, 678–680.

[57] **Yu, M.F.**, **Files, B.S.**, **Arepalli, S. and Ruoff, R.S.** (2000). Tensile Loading of Ropes of Single Wall Carbon Nanotubes and their Mechanical Properties, *Physical Review Letters*, *84*, 5552–5555.

[58] **Scarpa, F.**, **Adhikari, S.**, **Srikantha, A. and Phani** (2009). Effective elastic mechanical properties of single layer graphene sheets, *Nanotechnology*, *20*, 065709.

[59] **Lier, G.V.**, **Alsenoy, C.V.**, **Doren, V.V. and Geerlings, P.** (2000). Ab initio study of the elastic properties of single-walled carbon nanotubes and graphene, *Chemical Physics Letters*, *326*, 181–185.

[60] **Faccio, R.**, **Denis, P.A.**, **Pardo, H.**, **Goyenola, C. and Mombru, A.W.** (2009). Mechanical Properties of Graphene Nanoribbons, *Journal of Physics Condensed Matter*, *21*, 285304.

[61] **Tabarraei, A.**, **Shadalou, S. and Song, J.H.** (2015). Mechanical properties of graphene nanoribbons with disordered edges, *Computational Materials Science*, *96*, 10–19.

[62] **Tjong, S.C.** (2013). Recent progress in the development and properties of novel metal matrix nanocomposites reinforced with carbon nanotubes and graphene nanosheets, *Materials Science and Engineering R: Reports*, *74*, 281–350.

[63] **Silvestre, N.**, **Faria, B. and Lopes, J.N.C.** (2014). Compressive behavior of CNT-reinforced aluminum composites using molecular dynamics, *Composites Science and Technology*, *90*, 16–24.

[64] **Song, H.Y. and Zha, X.W.** (2010). Mechanical properties of nickel-coated single-walled carbon nanotubes and their embedded gold matrix composites, *Physics Letters, Section A: General, Atomic and Solid State Physics*, *374*, 1068–1072.

[65] **Song, H.Y. and Zha, X.W.** (2010). Influence of nickel coating on the interfacial bonding characteristics of carbon nanotube-aluminum composites, *Computational Materials Science*, *49*, 899–903.

[66] **Bashirvand, S. and Montazeri, A.** (2016). New aspects on the metal reinforcement by carbon nanofillers: A molecular dynamics study, *Materials and Design*, *91*, 306–313.

[67] **Guo, S.H.**, **Zhu, B.E.**, **Ou, X.D.**, **Pan, Z.Y. and Wang, Y.X.** (2010). Deformation of gold-filled single-walled carbon nanotubes under axial compression, *Carbon*, *48*, 4129–4135.

[68] **Tsai, P.C. and Jeng, Y.R.** (2013). Experimental and numerical investigation into the effect of carbon nanotube buckling on the reinforcement of CNT/Cu composites, *Composites Science and Technology*, *79*, 28–34.

[69] **Yoo, S.J.**, **Han, S.H. and Kim, W.J.** (2013). A combination of ball milling and high-ratio differential speed rolling for synthesizing carbon nanotube/copper composites, *Carbon*, *61*, 487–500.

[70] **Munir, K.S.**, **Kingshott, P. and Wen, C.** (2015). Carbon Nanotube Reinforced Titanium Metal Matrix Composites Prepared by Powder Metallurgy—A Review, *Critical Reviews in Solid State and Materials Sciences*, *40*, 38–55.

[71] **Deng, C.F.**, **Wang, D.Z.**, **Zhang, X.X. and Li, A.B.** (2007). Processing and properties of carbon nanotubes reinforced aluminum composites, *Materials Science and Engineering A*, *444*, 138–145.

[72] **Wang, J.**, **Li, Z.**, **Fan, G.**, **Pan, H.**, **Chen, Z. and Zhang, D.** (2012). Reinforcement with graphene nanosheets in aluminum matrix composites, *Scripta Materialia*, *66*, 594–597.

[73] **Rashad, M.**, **Pan, F.**, **Tang, A. and Asif, M.** (2014). Effect of Graphene Nanoplatelets addition on mechanical properties of pure aluminum using a semi-powder method, *Progress in Natural Science: Materials International*, *24*, 101–108.

[74] **Bartolucci, S.F.**, **Paras, J.**, **Rafiee, M.A.**, **Rafiee, J.**, **Lee, S.**, **Kapoor, D. and Koratkar, N.** (2011). Graphene-aluminum nanocomposites, *Materials Science and Engineering A*, *528*, 7933–7937.

[75] **Goh, C.S.**, **Wei, J.**, **Lee, L.C. and Gupta, M.** (2008). Ductility improvement and fatigue studies in Mg-CNT nanocomposites, *Composites Science and Technology*, *68*, 1432–1439.

[76] **Montazeri, A. and Rafii-Tabar, H.** (2011). Multiscale modeling of graphene- and nanotube-based reinforced polymer nanocomposites, *Physics Letters, Section A: General, Atomic and Solid State Physics*, *375*, 4034–4040.

[77] **Frankland, S.J.V.**, **Harik, V.M.**, **Odegard, G.M.**, **Brenner, D.W. and Gates, T.S.** (2003). The stress-strain behavior of polymer-nanotube composites from molecular dynamics simulation, *Composites Science and Technology*, *63*, 1655–1661.

[78] **Ebrahimi, S.**, **Ghafoori-Tabrizi, K. and Rafii-Tabar, H.** (2012). Multi-scale computational modelling of the mechanical behaviour of the chitosan biological polymer embedded with graphene and carbon nanotube, *Computational Materials Science*, *63*, 347–353.

[79] **Ercolessi, F.**, (1997). A molecular dynamics primer, ICTP.

[80] **Frenkel, D. and Smit, B.**, (1996). Understanding Molecular Simulation, Academic Press.

[81] **Daw, M.S. and Baskes, M.I.** (1984). Embedded-atom method: Derivation and application to impurities, surfaces, and other defects in metals, *Physical Review B*, *29*, 6443–6453.

[82] **Stuart, S.J.**, **Tutein, A.B. and Harrison, J.A.** (2000). A reactive potential for hydrocarbons with intermolecular interactions, *The Journal of Chemical Physics*, *112*, 6472–6486.

[83] **Brenner, D.W.**, **Shenderova, O.A.**, **Harrison, J.A.**, **Stuart, S.J.**, **Bi, B. and Sinnott, S.B.** (2002). A second-generation reactive empirical bond order (REBO) potential energy expression for hydrocarbons, *Journal of Physics: Condensed Matter*, *14*, 783–802.

[84] **Finney, J.L.** (1975). Volume occupation, environment and accessibility in proteins. The problem of the protein surface, *J. Mol. Biol.*, *96*, 721–732.

[85] **Zhu, H.X. and Windle, A.H.** (2002). Effects of cell irregularity on the high strain compression of open-cell foams, *Acta Mater.*, *50*, 1041–1052.

[86] **Zhu, H.X.**, , **Hobdell, J. and Windle, A.H.** (2000). Effects of cell irregularity on the elastic properties of open-cell foams, *Acta Mater.*, *48*, 4893–48900.

[87] **Getis, A. and Boots, B.**, (2008). Models of Spatial Processes:An Approach to the Study of Point, Line and Area Patterns, Cambridge University Press, New York.

[88] **Icke, V.** (1996). Particles, space, and time, *Astrophys. Space Sci.*, *244*, 293–311.

[89] **Yang, R.Y.**, **Zou, R.P. and Yu, A.B.** (2002). Voronoi tesellation of the packing of fine uniform spheres, *Physical Review E*, *65*, 041302.

[90] **Foiles, S.M.**, **Baskes, M.I. and Daw, M.S.** (1986). Embedded-atom-method functions for the fcc metals Cu, Ag, Au, Ni, Pd, Pt, and their alloys, *Physical Review B*, *33*, 7983–7991.

[91] **Plimpton, S.** (1995). Fast Parallel Algorithms for Short-Range Molecular Dynamics, *Journal of Physics: Condensed Matter*, *117*, 1–19.

[92] **Laboratories, S.N.**, `http://lammps.sandia.gov/`, accessed: 07 04 2017.

[93] **Stuart, S.J.**, **Tutein, A.B. and Harrison, J.A.** (2000). A reactive potential for hydrocarbons with intermolecular interactions, *The Journal of Chemical Physics*, *112*, 6472–6486.

[94] **Luedtke, W.D. and Landman, U.** (1999). Slip diffusion and Levy flights of an adsorbed gold nanocluster, *Physical Review Letters*, *82*, 3835–3838.

[95] **Thompson, A.P.**, **Plimpton, S.J. and Mattson, W.** (2009). General formulation of pressure and stress tensor for arbitrary many-body interaction potentials under periodic boundary conditions, *The Journal of Chemical Physics*, *131*, 154107.

[96] **Tsai, D.H.** (1979). The virial theorem and stress calculation in molecular dynamics, *J. Chem. Phys.*, *70*, 1375–1382.

CURRICULUM VITAE

Name Surname: Deniz Ezgi GÜLMEZ

Place and Date of Birth: Mersin, 02.02.1991

E-Mail: gulmez15@itu.edu.tr

EDUCATION:

- **B.Sc.:** 2014, Dokuz Eylul University, Faculty of Engineering, Department of Mechanical Engineering
- **M.Sc.:** 2017, Istanbul Technical University, Faculty of Mechanical Engineering, Department of Mechanical Engineering

PROFESSIONAL EXPERIENCE AND REWARDS:

- 2017- Istanbul Technical University-Research Asistant.
- 2015-2016 Istanbul Technical University-Project Student.

PUBLICATIONS, PRESENTATIONS AND PATENTS ON THE THESIS:

- Gülmez D. E., Kırca M., 2016. Nanoporous Metals Reinforced with Fullerenes. *18th International Conference - Theoretical and Applied Multiscale Mechanics*, August 04-05, 2016 Amsterdam, The Netherlands.